## Neutralization of IL-16 Ameliorates the Development of Cardiac Fibrosis

Chronic infusion of Ang II induces hypertension and cardiac fibrosis, and has been used as a model to explore the mechanisms underlying the fibrotic process in the heart. Using this model, we examined the effect of IL-16 neutralization on cardiac fibrosis. After 14 days of Ang II infusion, IL-16 mRNA was significantly upregulated in the LV myocardium (Figure 7A). Neutralization of IL-16 had no effect on IL-16 mRNA levels, suggesting that neutralization of IL-16 neither promotes nor suppresses IL-16 expression in cardiac tissue (Figure 7A). Histopathology of the heart from the mice infused with Ang II for 28 days showed marked cardiac fibrosis, which was significantly attenuated by anti-IL-16 neutralizing antibody therapy without any effect on systemic blood pressure (Table 6 and Figure 7B). Atrial weight and lung weight were also decreased by IL-16 neutralization, suggesting that IL-16 neutralization might have inhibited the increase in LV filling pressure and pulmonary congestion (Table 6).

## Discussion

Serum IL-16 levels were elevated in both HFpEF patients and the HFpEF rat model, and closely associated with parameters of LV diastolic dysfunction and LV stiffening. Cardiac expression of IL-16 was augmented in the HFpEF rats. Cardiac-enhanced expression of IL-16 in mice promoted LV fibrosis and LV myocardial stiffening in proportion with IL-16 expression levels. Neutralization of IL-16 ameliorated cardiac fibrosis in the mouse model of Ang II-induced hypertension.

IL-16 was first described as a T-cell chemoattractant generated from human peripheral blood mononuclear cells [40]. Since then, IL-16 has been shown to be associated with various inflammatory, allergic or infectious diseases [19–21], but the role of IL-16 in the pathophysiology of heart failure has not been previously reported. In the present study, we showed the first evidence that IL-16 mediates cardiac inflammation leading to increased cardiac fibrosis and LV stiffness. Moreover, serum IL-16 levels were elevated in HFpEF patients compared with the control group but not in HFrEF patients, suggesting that IL-16 might be a specific inflammatory mediator associated with the development of HFpEF.

In the LV myocardium of IL-16 TG mice, we found a significant increase in macrophages, which has been previously suggested to be involved in the development of cardiac fibrosis [17,37,38]. However, we did not find an increase in T-cells (data not shown). This was unexpected since CD4 has been reported to be the primary cell surface receptor for IL-16, and increased infiltration of CD4+ T-cells has been reported at the site of IL-16-mediated inflammation [20]. IL-16 has also been reported to use receptors other than CD4 [41], but we could not identify the

receptor responsible for IL-16-mediated chemoattraction of macrophages into the heart. Although it is likely that IL-16 secreted in the heart causes infiltration of macrophages into the myocardium, further investigation is needed to clarify the difference in IL-16-induced chemoattraction of cells between the heart and other organs.

IL-16 has been shown to induce the production of several cytokines and chemokines from monocytes/macrophages [42], but this is the first report to demonstrate that IL-16 promotes the release of the profibrotic cytokine TGF-β1 from macrophages. Therefore, our results suggest that IL-16 might promote cardiac fibrosis in HFpEF through chemoattraction of macrophages into the myocardium and subsequent stimulation of the release of TGF-β1 from macrophages. Blocking the effect of IL-16 might inhibit this pathway, resulting in the amelioration of cardiac fibrosis and reduced LV stiffness.

Recently, we have reported that a decreased DWS, which is calculated from the movement of the epicardial edge of the LV free wall during diastole, reflects LV wall stiffening [23] and predicts a poor outcome in HFpEF patients [26]. In this study, we found a correlation between serum IL-16 levels and DWS in human subjects, suggesting an association between serum IL-16 levels and LV myocardial stiffness. In addition, we found a correlation between serum IL-16 levels and MSC in rats, suggesting a similar association between IL-16 and LV myocardial stiffness. This study suggested that the elevation of circulating levels of IL-16 in HFpEF could not be explained by the overexpression of IL-16 in the heart, and failed to clarify the source for the elevation; however, measurement of circulating levels of IL-16 might be useful as a surrogate biomarker for estimating the extent of LV myocardial stiffening in HFpEF patients and for risk stratification of patients with HFpEF. Future clinical studies with a larger number of subjects are required to investigate this hypothesis.

In summary, our present work provides the first evidence that IL-16 mediates cardiac inflammation leading to increased cardiac fibrosis and LV stiffness in HFpEF. Blockade of IL-16 may be a possible therapeutic strategy to treat HFpEF.

## Acknowledgments

## Author Contributions

Conceived and designed the experiments: ST T. Mano YS TO T. Miwa KY IK. Performed the experiments: ST Y. Takeda DK YO Y. Tsukamoto YI AK M. Kawai KH RI MH M. Kaneko HH. Analyzed the data: ST T. Mano YS TO KY. Contributed reagents/materials/analysis tools: RI MH M. Kaneko. Wrote the paper: ST T. Mano KY IK.

## References

1. Roger VL, Weston SA, Redfield MM, Hellermann-Homan JP, Killian J, et al. (2004) Trends in heart failure incidence and survival in a community-based population. JAMA 292: 344 350.
2. Bhatia RS, Tu JV, Lee DS, Austin PC, Fang J, et al. (2006) Outcome of heart failure with preserved ejection fraction in a population based study. N Engl J Med 355: 260 269.
3. Owan TE, Hodge DO, Herges RM, Jacobsen SJ, Roger VL, et al. (2006) Trends in prevalence and outcome of heart failure with preserved ejection fraction. N Eng J Med 355: 251 259.
4. Yusuf S, Pfeffer MA, Swedberg K, Granger CB, Held P, et al. (2003) Effects of candesartan in patients with chronic heart failure and preserved left-ventricular ejection fraction: the CHARM-Preserved Trial. Lancet 362: 777 781.
5. Zile MR, Baicu CF, Gaasch WH (2004) Diastolic heart failure abnormalities in active relaxation and passive stiffness of the left ventricle. N Engl J Med 350: 1953 1959.
6. Yamamoto K, Masuyama T, Sakata Y, Nishikawa N, Mano T, et al. (2002) Myocardial stiffness is determined by ventricular fibrosis, but not by compensatory or excessive hypertrophy in hypertensive heart. Cardiovasc Res 55: 76 82.
7. Masuyama T, Yamamoto K, Sakata Y, Doi R, Nishikawa N, et al. (2000) Evolving changes in Doppler mitral flow velocity pattern in rats with hypertensive hypertrophy. J Am Coll Cardio. 36: 2333 2338.
8. Anker SD, von Haehling S (2004) Inflammatory mediators in chronic heart failure: an overview. Heart 90: 464 470.
9. Mann DL (2002) Inflammatory mediators and the failing heart: past, present, and the foreseeable future. Circ Res 91: 988 998.
10. Aukrust P, Ueland T, Muller F, Andreassen AK, Nordoy I, et al. (1998) Elevated circulating levels of C-C chemokines in patients with congestive heart failure. Circulation 97: 1136 1143.

66

11. Deswal A, Petersen NJ, Feldman AM, Young JB, White BG, et al. (2001) Cytokines and cytokine receptors in advanced heart failure: an analysis of the cytokine database from the Vesnarinone trial (VEST). Circulation 103: 2055 2059.

12. Yu Q, Vazquez R, Khojeini EV, Patel C, Venkataramani R, et al. (2009) IL 18 induction of osteopontin mediates cardiac fibrosis and diastolic dysfunction in mice. Am J Physiol Heart Circ Physiol 297: H76 85.

13. Melendez GC, McLarty JL, Levick SP, Du Y, Janicki JS, et al. (2010) Interleukin 6 mediates myocardial fibrosis, concentric hypertrophy, and diastolic dysfunction in rats. Hypertension 56: 225 231.

14. Cieslik KA, Taffet GE, Carlson S, Hermosillo J, Trial J, et al. (2011) Immune-inflammatory dysregulation modulates the incidence of progressive fibrosis and diastolic stiffness in the aging heart. J Mol Cell Cardiol 50: 248 256.

15. Wynn TA (2007) Common and unique mechanisms regulate fibrosis in various fibroproliferative diseases. J Clin Invest 117: 524 529.

16. Berk BC, Fujiwara K, Lehoux S (2007) ECM remodeling in hypertensive heart disease. J Clin Invest 117: 568 575.

17. Yoshida J, Yamamoto K, Mano T, Sakata Y, Nishikawa N, et al. (2004) AT1 receptor blocker added to ACE inhibitor provides benefits at advanced stage of hypertensive diastolic heart failure. Hypertension 43: 686 691.

18. Westermann D, Lindner D, Kasner M, Zietsch C, Savvatis K, et al. (2011) Cardiac inflammation contributes to changes in the extracellular matrix in patients with heart failure and normal ejection fraction. Circ Heart Fail 4: 44 52.

19. Keates AC, Castagliuolo I, Cruickshank WW, Qiu B, Arseneau KO, et al. (2000) Interleukin 16 is up-regulated in Crohn's disease and participates in TNBS colitis in mice. Gastroenterology 119: 972 982.

20. Skundric DS, Cai J, Cruikshank WW, Gveric D (2006) Production of IL-16 correlates with CD4+ Th1 inflammation and phosphorylation of axonal cytoskeleton in multiple sclerosis lesions. J Neuroinflammation 3: 13.

21. Hessel EM, Cruikshank WW, Van Ark I, De Bie JJ, Van Esch B, et al. (1998) Involvement of IL-16 in the induction of airway hyper-responsiveness and up-regulation of IgE in a murine model of allergic asthma. J Immunol 160: 2998 3005.

22. McKee PA, Castelli WP, McNamara PM, Kannel WB (1971) The natural history of congestive heart failure: the Framingham study. N Engl J Med 285: 1441 1446.

23. Takeda Y, Sakata Y, Higashimori M, Mano T, Nishio M, et al. (2009) Noninvasive assessment of wall distensibility with the evaluation of diastolic epicardial movement. J Card Fail 15: 68 77.

24. Lang RM, Bierig M, Devereux RB, Flachskampf FA, Foster E, et al. (2005) Recommendations for chamber quantification: a report from the American Society of Echocardiography's Guidelines and Standards Committee and the Chamber Quantification Writing Group, developed in conjunction with the European Association of Echocardiography, a branch of the European Society of Cardiology. J Am Soc Echocardiogr 18: 1440 1463.

25. Lester SJ, Ryan EW, Schiller NB, Foster E (1999) Best method in clinical practice and in research studies to determine left atrial size. Am J Cardiol 84: 829 832.

26. Ohtani T, Mohammed SF, Yamamoto K, Dunlay SM, Weston SA, et al. (2012) Diastolic stiffness as assessed by diastolic wall strain is associated with adverse remodelling and poor outcomes in heart failure with preserved ejection fraction. Eur Heart J 33: 1742 1749.

27. Kamimura D, Ohtani T, Sakata Y, Mano T, Takeda Y, et al. (2012) Ca$^{2+}$ entry mode of Na$^+$/Ca$^{2+}$ exchanger as a new therapeutic target for heart failure with preserved ejection fraction. Eur Heart J 33: 1408 1416.

28. Meagher C, Beilke J, Arreaza G, Mi QS, Chen W, et al. (2010) Neutralization of interleukin-16 protects nonobese diabetic mice from autoimmune type 1 diabetes by a CCL4-dependent mechanism. Diabetes 59: 2862 2871.

29. Kimura N, Itoh S, Nakae S, Axtell RC, Velotta JB, et al. (2011) Interleukin-16 deficiency suppresses the development of chronic rejection in murine cardiac transplantation model. J Heart Lung Transplant 30: 1409 1417.

30. Terui T, Shimamoto Y, Yamane M, Kobirumaki F, Ohtsuki I, et al. (2010) Regulatory mechanism of length-dependent activation in skinned porcine ventricular muscle: role of thin filament cooperative activation in the Frank-Starling relation. J Gen Physiol 136: 469 482.

31. Ishii R, Higashimori M, Tadakuma K, Kaneko M, Tamaki S, et al. (2011) Balloon type elasticity sensing for left ventricle of small laboratory animal. Conf Proc IEEE Eng Med Biol Soc 2011: 904 907.

32. Ohtani T, Mano T, Hikoso S, Sakata Y, Nishio M, et al. (2009) Cardiac steroidogenesis and glucocorticoid in the development of cardiac hypertrophy during the progression to heart failure. J Hypertens 27: 1074 1083.

33. Xu J, Carretero OA, Liao TD, Peng H, Shesely EG, et al. (2010) Local angiotensin II aggravates cardiac remodeling in hypertension. Am J Physiol Heart Circ Physiol 299: H1328 1338.

34. Shimoyama M, Hayashi D, Takimoto E, Zou Y, Oka T, et al. (1999) Calcineurin plays a critical role in pressure overload-induced cardiac hypertrophy. Circulation 100: 2449 2454.

35. Doser TA, Turdi S, Thomas DP, Epstein PN, Li SY, et al. (2009) Transgenic overexpression of aldehyde dehydrogenase-2 rescues chronic alcohol intake-induced myocardial hypertrophy and contractile dysfunction. Circulation 119: 1941 1949.

36. Maurer MS, Burkhoff D, Fried LP, Gottdiener J, King DL, et al. (2007) Ventricular structure and function in hypertensive participants with heart failure and a normal ejection fraction: the Cardiovascular Health Study. J Am Coll Cardiol 49: 972 981.

37. Moriwaki H, Stempien-Otero A, Kremen M, Cozen AE, Dichek DA (2004) Overexpression of urokinase by macrophages or deficiency of plasminogen activator inhibitor type 1 causes cardiac fibrosis in mice. Circ Res 95: 637 644.

38. Hinglais N, Heudes D, Nicoletti A, Mandet C, Laurent M, et al. (1994) Colocalization of myocardial fibrosis and inflammatory cells in rats. Lab Invest 70: 286 294.

39. Cruikshank WW, Berman JS, Theodore AC, Bernardo J, Center DM (1987) Lymphokine activation of T4+ T lymphocytes and monocytes. J Immunol 138: 3817 3823.

40. Center DM, Cruikshank W (1982) Modulation of lymphocyte migration by human lymphokines. I. Identification and characterization of chemoattractant activity for lymphocytes from mitogen-stimulated mononuclear cells. J Immunol 128: 2563 2568.

41. Cruikshank W, Little F (2008) Interleukin-16: the ins and outs of regulating T-cell activation. Crit Rev Immunol 28: 467 483.

42. Hermann E, Darcissac E, Idziorek T, Capron A, Bahr GM (1999) Recombinant interleukin 16 selectively modulates surface receptor expression and cytokine release in macrophages and dendritic cells. Immunology 97: 241 248.

67

# Circulation

American
Heart
Association®

## Enhanced Survival of Transplanted Human Induced Pluripotent Stem Cell–Derived Cardiomyocytes by the Combination of Cell Sheets With the Pedicled Omental Flap Technique in a Porcine Heart

Masashi Kawamura, Shigeru Miyagawa, Satsuki Fukushima, Atsuhiro Saito, Kenji Miki, Emiko Ito, Nagako Sougawa, Takuji Kawamura, Takashi Daimon, Tatsuya Shimizu, Teruo Okano, Koichi Toda and Yoshiki Sawa

The online version of this article, along with updated information and services, is located on the
World Wide Web at:
http://circ.ahajournals.org/content/128/11_suppl_1/S87

# Enhanced Survival of Transplanted Human Induced Pluripotent Stem Cell–Derived Cardiomyocytes by the Combination of Cell Sheets With the Pedicled Omental Flap Technique in a Porcine Heart

Masashi Kawamura, MD; Shigeru Miyagawa, MD, PhD; Satsuki Fukushima, MD, PhD;
Atsuhiro Saito, PhD; Kenji Miki, PhD; Emiko Ito, PhD; Nagako Sougawa, PhD;
Takuji Kawamura, MD; Takashi Daimon, PhD; Tatsuya Shimizu, MD, PhD; Teruo Okano, PhD;
Koichi Toda, MD, PhD; Yoshiki Sawa, MD, PhD

***Background***—Transplantation of cardiomyocytes that are derived from human induced pluripotent stem cell–derived cardiomyocytes (hiPS-CMs) shows promise in generating new functional myocardium in situ, whereas the survival and functionality of the transplanted cells are critical in considering this therapeutic impact. Cell-sheet method has been used to transplant many functional cells; however, potential ischemia might limit cell survival. The omentum, which is known to have rich vasculature, is expected to be a source of blood supply. We hypothesized that transplantation of hiPS-CM cell sheets combined with an omentum flap may deliver a large number of functional hiPS-CMs with enhanced blood supply.

***Methods and Results***—Retrovirally established human iPS cells were treated with Wnt signaling molecules to induce cardiomyogenic differentiation, followed by superparamagnetic iron oxide labeling. Cell sheets were created from the magnetically labeled hiPS-CMs using temperature-responsive dishes and transplanted to porcine hearts with or without the omentum flap (n=8 each). Two months after transplantation, the survival of superparamagnetic iron oxide–labeled hiPS-CMs, assessed by MRI, was significantly greater in mini-pigs with the omentum than in those without it; histologically, vascular density in the transplanted area was significantly greater in mini-pigs with the omentum than in those without it. The transplanted tissues contained abundant cardiac troponin T–positive cells surrounded by vascular-rich structures.

***Conclusions***—The omentum flap enhanced the survival of hiPS-CMs after transplantation via increased angiogenesis, suggesting that this strategy is useful in clinical settings. The combination of hiPS-CMs and the omentum flap may be a promising technique for the development of tissue-engineered vascular-rich new myocardium in vivo. (***Circulation***. 2013;128[suppl 1]:S87-S94.)

**Key Words:** cell transplantation ■ induced pluripotent stem cells ■ regeneration

Stem cell therapy shows promise in the treatment of heart failure. However, the therapeutic benefits proven by clinical studies in the past decade were only modest, indicating that further investigations and refinements are required to establish this treatment in the clinical arena.[1,2] The success of cell transplantation therapy for heart failure is dependent on the choice of cell source, cell delivery method, and target cardiac pathology. In these previous clinical trials, transplantation of somatic tissue–derived stem or progenitor cells has shown no or low cardiomyogenic differentiation capacity in vivo, but contributed to functional recovery via paracrine effects, potentially limiting the therapeutic effects, in particular, in

treating severe heart failure.[1–4] In addition, it has been shown that direct intramyocardial or intracoronary injection of dissociated single cells, which was used in most of the clinical studies, yields <10% of engraftment rate of the cells immediately after transplantation, indicating that further refinement of the cell delivery method would be required to increase cell engraftment and enhance the consequent therapeutic effects.[1,2]

Human induced pluripotent stem (hiPS) cells are initially established by nuclear reprogramming of somatic cells.[5,6] hiPS cell carries a capacity of unlimited proliferation and differentiation to cardiomyocyte.[7] Transplantation of hiPS-derived cardiomyocytes (hiPS-CMs) would have, thus, a potential to

*Circulation* is available at http://circ.ahajournals.org  DOI: 10.1161/CIRCULATIONAHA.112.000366

increase the functional cardiomyocytes in damaged heart tissue to mechanically contribute to cardiac function. In addition, the recently developed scaffoldless tissue engineering technique of cell-sheet engineering is applicable to myocardial regeneration therapy.[8] This technique preserves extracellular matrix without artificial scaffolds, which may prevent cell detachment–associated anoikis.[9] In contrast to the needle injection technique, the cell-sheet technique can deliver a large number of cells to the damaged myocardium without loss of transplanted cells or injury to the host myocardium.[10,11] Importantly, this method has already shown feasibility and safety in the clinical study.[12] On these bases, we studied the therapeutic efficacy of transplantation of hiPS-CMs with the cell-sheet method in a porcine chronic ischemic cardiomyopathy model.[13] This study, however, showed that the transplanted cells rarely survived in the heart long-term, possibly because of poor vascular network support from the native tissue.

The omentum has been historically used in surgical revascularization for patients with ischemic heart disease[14–16] and is also known to have rich vasculature and angiogenic factors.[17,18] Importantly, we reported that a pedicle omentum flap covering the transplanted skeletal myoblast cell sheets enhanced angiogenesis over the cell-sheet–transplanted territory, survival of cells, and therapeutic effects.[19] We herein hypothesized that covering with an omentum flap may enhance the survival of transplanted hiPS-CM cell sheets via the promotion of angiogenesis over the transplanted territory. In this study, we compared the survival of hiPS-CMs, with or without a pedicle omentum flap, after transplantation to the mini-pig heart, and we examined whether the omentum enhanced the angiogenic capacity of hiPS-CM sheets in vivo.

## Materials and Methods

All experimental procedures were approved by the institutional ethics committee. Animal care was conducted humanely in compliance with the Principles of Laboratory Animal Care formulated by the National Society for Medical Research and the Guide for the Care and Use of Laboratory Animals prepared by the Institute of Animal Resources and published by the National Institutes of Health (publication no. 85-23, revised 1996).

### Preparation of SPIO-Labeled hiPS-CM Cell Sheets

The hiPS cell line 201B7 that was generated using the 4 transcription factors Oct4, Sox2, Klf4, and c-Myc was used in this study.[5] Culture of the hiPS cells, formation of the embryoid bodies, and subsequent cardiomyogenic differentiation and purification were performed as described previously to generate hiPS-CMs.[13] The purified hiPS-CMs were then labeled with the superparamagnetic iron oxide (SPIO) ferucarbotran (Resovist; Bayer Pharma, Berlin, Germany) using the hemagglutinating virus of Japan envelope vector (GenomOne-Neo; Ishihara Sangyo, Osaka, Japan).[20,21] Subsequently, human mesenchymal stem cells (Lonza, Basel, Switzerland) were seeded at a density of $5 \times 10^6$ cells/dish onto 10-cm UpCell dishes, on which the SPIO-labeled hiPS-CMs were grown. The next day, the dishes were incubated at room temperature, which induced the cells to detach spontaneously to form scaffold-free hiPS-CM cell sheets.

### Flow Cytometry

Dissociated cells after hiPS cell differentiation were fixed, permeabilized, and labeled with anticardiac isoform of troponin T (cTNT; clone 13211; Thermo Fisher scientific, Runcorn, UK) conjugated with Alexa-488 using Zenon technology (Invitrogen), followed by

analysis on BD FACSCanto II (BD Biosciences) with BD FACSDiva Software (BD Biosciences).

### Study Protocol

Normal 16 female mini-pigs (Japan Farm Co Ltd, Kagoshima, Japan) weighing 20 to 25 kg were randomly divided into 2 groups (n=8 each) to perform hiPS-CM cell-sheet transplantation either with or without the pedicle omentum translocation. All animals were immunosuppressed by daily administration of tacrolimus (0.75 mg/kg; Astellas, Tokyo, Japan), mycophenolate mofetil (500 mg; Teva Czech Industries s.r.o, Opava, Czech), and prednisolone (20 mg; Takeda Pharmaceutical Co Ltd, Osaka, Japan) daily from 5 days before transplantation until euthanasia. Cardiac MRI scans were taken on the same mini-pigs at 1 week, 4 weeks, and 8 weeks after transplantation. After the final scan, the mini-pigs were humanely euthanized for analysis (Figure 1A).

### Transplantation of SPIO-Labeled hiPS-CM Cell Sheets Covered With the Pedicle Omentum

All animals were preanesthetized with ketamine hydrochloride (20 mg/kg; Daiichi Sankyo, Tokyo, Japan) and xylazine (2 mg/kg; Bayer HealthCare, Leverkusen, Germany), intubated endotracheally, and maintained by continuous infusion of propofol (6 mg/kg per hour; AstraZeneca K.K., Osaka, Japan) and vecuronium bromide (0.05 mg/kg per hour; Daiichi Sankyo). Seven SPIO-labeled hiPS-CM sheets were placed on the epicardium via the median sternotomy. In the case of transplantation of the cell sheet covered with the pedicled omentum, the omentum was mobilized to the mediastinal space via additional small upper midline laparotomy, preserving both gastroepiploic arteries and their arcade. Initially, 4 hiPS-CM cell sheets were placed on the epicardium and covered with the omentum. The remaining 3 hiPS-CM cell sheets, then, were placed on the covering omentum and covered with the omentum again (Figure 1B). The omentum was stitched and fixed on the excised pericardium (Figure 1C). Mini-pigs were then allowed to recover and were later humanely euthanized.

### Cardiac MRI

ECG-gated cardiac MRI (CMR) was performed under general anesthesia with an 8-channel cardiac coil wrapped around the chest wall.[22] CMR images were acquired on a 1.5-T MR scanner (Signa EXCITE XI TwinSpeed; GE Medical Systems, Milwaukee, WI). To assess SPIO-labeled hiPS-CM detection, animals were imaged 1 week after transplantation. In addition, 1 animal was reimaged at 4 and 8 weeks after transplantation to detect SPIO-labeled hiPS-CM retention. Short-axis images with 8-mm slice thickness, including the entire heart, were obtained by pulse parameters for cardiac-gated, fast gradient–recalled echo. The SPIO-labeled hiPS-CM hypointense area was measured using planimetry of fast gradient–recalled echo images on a workstation (Virtual Place Lexus64; AZE, Tokyo, Japan). The survival proportion of hiPS-CMs was determined using the hypointense area at 4 and 8 weeks after transplantation divided by the area at 1 week after transplantation as the baseline.

### Histology and Immunohistolabeling

The hiPS-CM cell sheets and the excised heart specimens were either embedded in paraffin or optimal cutting temperature compound (Tissueb Tek; Sakura Finetek, Torrance, CA) for frozen section. The paraffin-embedded sections were stained with hematoxylin-eosin or Prussian blue that visualizes iron contents. Ten different fields were randomly selected. The number of spindle-shaped cells with a nucleus and iron in the cytoplasm in each field was counted with a light microscopy under high-power magnification (×400). Cells from 10 fields were averaged, and the results are expressed as cell density (per high-power field). In addition, the paraffin-embedded sections were immunolabeled with anti-human von Willebrand factor antibody (Dako, Glostrup, Denmark) and visualized with the horseradish peroxidase-based EnVision kit (Dako). Ten different fields were randomly selected, and the number of von Willebrand factor–positive
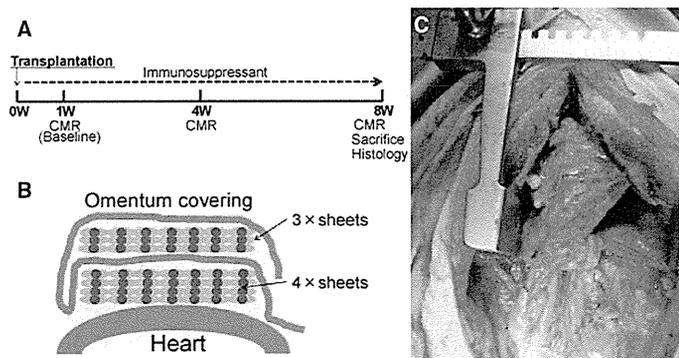
Figure 1. Study protocol of the mini-pig experiment and operative procedure. A, Schedule of cardiac MRI (CMR) and histological evaluations. B, Procedural scheme of cell-sheet transplantation with the omentum. C, Image taken after treatment. The omentum is mobilized and transplanted with the cell sheets on the heart through median sternotomy with an additional upper midline laparotomy.

cells in each field was counted using a light microscope under high-power magnification (×200). The stained blood vessels from the 10 fields were averaged and the results expressed as vascular density (per square millimeter). The frozen sections were immunolabeled with anti-cTNT antibody (1:100 dilution; Abcam, Cambridge, UK) and anti-CD68 antibody for macrophages (1:100 dilution, Abcam) as primary antibodies and visualized with AlexaFluor488–conjugated goat anti-mouse (Invitrogen) and AlexaFluor555–conjugated goat anti-rabbit (Invitrogen) as secondary antibodies. Nuclei were counterstained with 4′,6-diamidino-2-phenylindole (Dojindo, Tokyo, Japan) and assessed using the Biorevo BZ-9000 (Keyence) or confocal microscopy (Olympus Japan, FV1000-D IX81, Tokyo, Japan). SPIO particles of Prussian blue staining were visualized by differential interference contrast of confocal microscopy.

### Real-Time Polymerase Chain Reaction

Total RNA was extracted from cardiac tissue and reverse transcribed using Omniscript reverse transcriptase (Qiagen, Hilden, Germany) with random primers (Invitrogen), and the resulting cDNA was used for real-time polymerase chain reaction with the ABI PRISM 7700 (Applied Biosystems, Stockholm, Sweden) system using pig-specific primers (Applied Biosystems) for vascular endothelial growth factor (VEGF), basic fibroblast growth factor, and stromal-derived factor-1 (SDF-1). Each sample was analyzed in triplicate for each gene studied. Data were normalized to GAPDH expression level. For relative expression analysis, the delta-delta Ct method was used, and values of the cell-sheet transplantation without the omentum were used as reference values.

### Statistical Analysis

Data are expressed as means±SDs. Comparisons between 2 groups were made using Welch *t* test. Cell survival proportion over time was assessed by repeated-measures ANOVA with group, time, and group×time interaction effects. All *P* values are 2-sided, and values of *P*<0.05 were considered to indicate statistical significance. Statistical analyses were performed using JMP 9.02 (SAS Institute, Cary, NC).

## Results

### Generation of SPIO-Labeled hiPS-CM Cell Sheets

Cardiomyogenic differentiation of hiPS cells was induced by treatment of the embryoid bodies formed from cultured hiPS cells with Wnt3a and R-spondin-1. Subsequently, the differentiated hiPS cells were purified by culture in glucose-free medium to yield ≈1 to 2×10⁷ hiPS-CMs. Approximately 80% (83.6±8.1%) of the hiPS-CMs were positive for cTNT, as determined by flow cytometry (Figure 2A). After SPIO labeling to the hiPS-CMs, human mesenchymal stem cells were added

to the hiPS-CM culture. Subsequently, culture in the thermoresponsive dishes yielded round-shaped hiPS-CM cell sheets (Figure 2B). The hiPS-CMs on the sheet continued to beat before and after detaching from culture surface (Movies I and II in the online-only Data Supplement). Immunohistolabeling showed that the large number of cells in the hiPS-CM cell sheets were homogeneously positive for cTNT (Figure 2C). Prussian blue staining confirmed that the hiPS-CMs contained iron in the cytoplasm (Figure 2D).

### In Vivo Analysis of Survival of Transplanted SPIO-Labeled hiPS-CMs by Serial CMR

Transplantation of the same number of hiPS-CM cell sheets with or without the omentum covering was successfully performed via median sternotomy in 16 normal mini-pigs. There was no mortality related to the procedure or otherwise before the planned euthanasia. In addition, the omentum was attached to the surface of the heart in all mini-pigs with the omentum. CMRs were performed to assess the survival of transplanted SPIO-labeled hiPS-CMs at 1 week (baseline), 4 weeks, and 8 weeks after cell transplantation.

SPIO signals were clearly identified as the hypointense area in the surface of the left ventricle by CMR in all mini-pigs throughout the study period (Figure 3A). SPIO-positive hypointense area was gradually decreased in both the groups during the 8 weeks, whereas the SPIO-positive area was larger and thicker in mini-pigs with the omentum compared with those without the omentum during the study period. The survival proportion of the SPIO-labeled hiPS-CMs was determined by the formula that the hypointense area at 4 and 8 weeks after transplantation was divided by the area at 1 week after transplantation as baseline. Both groups showed steady decrease in the cell survival during the 7 weeks, whereas the proportion of decrease was significantly less in mini-pigs with the omentum than in those without it at 4 weeks (92±10% versus 60±10%) and 8 weeks (78±10% versus 42±9%) after treatment (*P*<0.0001 for interaction effect of time and group in the repeated ANOVA; Figure 3B).

### Histological Evaluation of Transplanted hiPS-CMs With or Without the Omentum

Excised heart tissues at 8 weeks after transplantation were assessed by histology. The transplanted hiPS-CMs and the
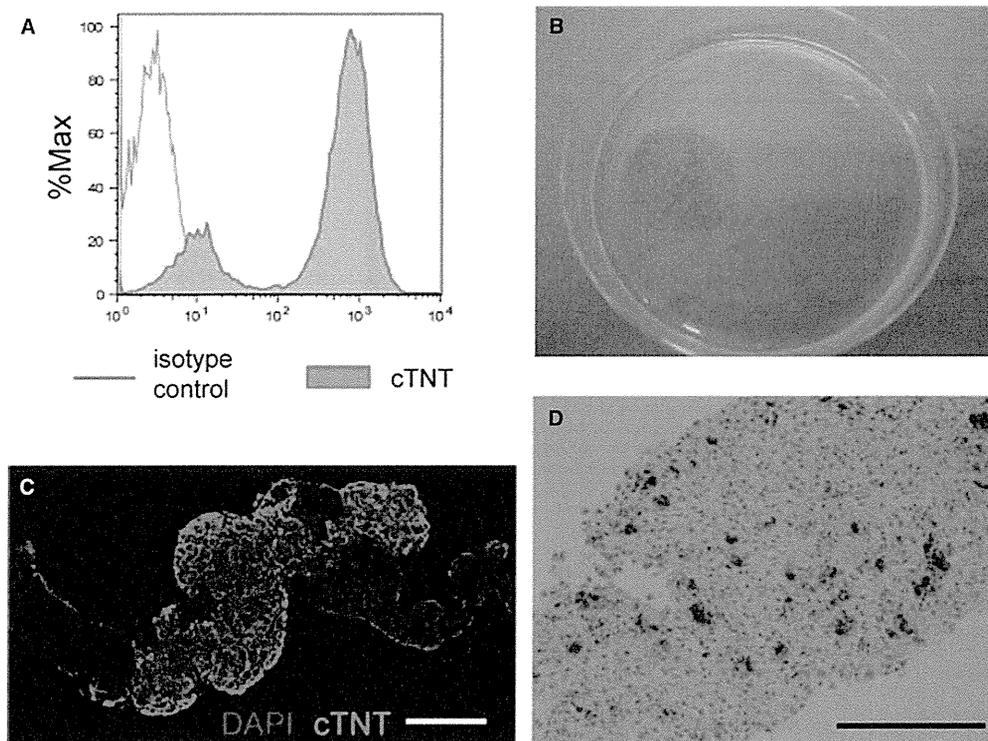
Figure 2. Histological characteristics of the human induced pluripotent stem cell–derived cardiomyocyte (hiPS-CM) cell sheet. A, Expression of cardiac troponin T (cTNT) after differentiation and purification of hiPS-CMs. B, A superparamagnetic iron oxide (SPIO)–labeled hiPS-CM cell sheet in a 10-cm dish. C, Immunostaining of the hiPS-CM cell sheet with cTNT antibody (green). The cell nuclei were counterstained with 4′,6-diamidino-2-phenylindole (DAPI; blue). D, Prussian blue staining of the SPIO-labeled hiPS-CM cell sheet. Scale bar, 50 μm in C and D.

pedicle omentum were attached over the epicardium of the left ventricle without any histological gaps in all mini-pigs, as assessed by hematoxylin–eosin staining (Figure 4D). The hearts without the omentum showed cellular and fibrous components over the anterior wall of the ventricles (Figure 4A), whereas the hearts with the omentum showed thick cellular, fibrous, and fat-rich components covering the anterior and lateral wall of the ventricles (Figure 4D).

Prussian blue staining revealed cells containing iron on the surface of the ventricles, corresponding to the area seen on CMR in both groups (Figure 4B and 4E). A larger number of cells with iron contents were identified in mini-pigs with the omentum compared with those without (Figure 4B, 4C, 4E, and 4F). In fact, the density of iron-containing cells in the transplanted site, assessed semiquantitatively by Prussian blue staining at 8 weeks after treatment, was significantly greater in the mini-pig with the omentum (27±6 cells/high-power field) than in those without it (5±2 cells/high-power field; $P<0.0001$; Figure 4G). Immunohistolabeling showed that a larger number of cells are positive for cTNT in the area where cells with iron inclusions are present in mini-pigs with the omentum compared with those without it (Figure 4H). The distribution of the SPIO particles was visualized by

differential interference contrast of confocal microscopy. Grafted hiPS-CMs were identified and confirmed as double-positive for cTNT and SPIO and negative for CD68, which is a specific marker for macrophages, by immunohistolabeling (Figure 4I–4N). In addition, no teratomas were formed in the heart or other thoracic organs at 8 weeks after the transplantation of the hiPS-CM cell sheets with or without the omentum (data not shown).

## Capillary Density in the Transplanted Area

Vessels and capillaries in the transplanted cell sheets at 8 weeks after transplantation were visualized and assessed by immunohistochemistry for von Willebrand factor. The transplanted cell sheets without the omentum contained a large number of capillaries and a small number of vessels in a homogeneous manner (Figure 5A), suggesting that vascular network was created possibly to support the survival and function of the cell sheets. Of note, the number of capillaries and vessels were markedly greater in the cell sheets covered by the omentum compared with those without it (Figure 5B). In fact, capillary density in the transplanted cell sheets, assessed semiquantitatively by immunohistochemistry for von Willebrand factor at 8 weeks after treatment, was significantly and markedly
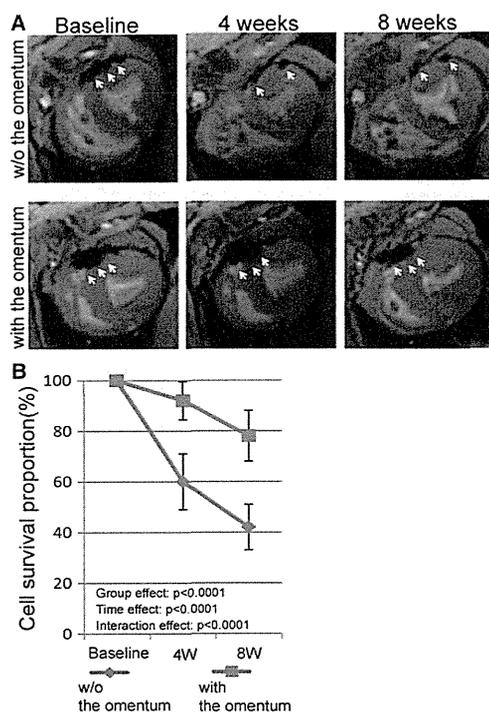
Figure 3. In vivo analysis of the survival of superparamagnetic iron oxide (SPIO)–labeled human induced pluripotent stem cell–derived cardiomyocytes (hiPS-CMs) after transplantation. A, Serial cardiac MRIs were examined at 1 week (baseline), 4 weeks, and 8 weeks after SPIO-labeled hiPS-CM cell-sheet transplantation, with or without the omentum. Representative hypointense area of the SPIO-labeled hiPS-CMs is indicated by white arrows. B, Cell survival proportion was estimated by the SPIO-labeled area at 4 and 8 weeks, corrected by cell survival at 1 week.

greater in mini-pigs with the omentum (64±21 U/mm$^2$) than in those without it (9±5 U/mm$^2$; $P<0.0001$; Figure 5C).

## Upregulation of VEGF, Basic Fibroblast Growth Factor, and SDF-1 Expression in the Transplanted Area

The expression level of cardioprotective and angiogenic factors in the transplanted area at 8 weeks after treatment was quantitatively assessed by real-time polymerase chain reaction for VEGF, basic fibroblast growth factor, and SDF-1. The relative expression of all the factors in the transplanted area was significantly greater in mini-pigs with the omentum than in those without it (VEGF, 1.94±0.38 versus 1.35±0.26; $P<0.05$; basic fibroblast growth factor, 2.33±0.92 versus 1.21±0.19; $P<0.05$; SDF-1, 2.05±0.33 versus 1.22±0.21; $P<0.01$; Figure 6A–6C).

## Discussion

It is herein demonstrated that our differentiation protocol yielded hiPS-CMs with >80% purity, and hiPS-CM cell sheets were transplanted over the anterior wall of the ventricle,

covered by the pedicle omentum, in a porcine model without procedural failure or procedure-related morbidity/mortality. The number of surviving cTNT-positive hiPS-CMs on the native myocardium was significantly greater in mini-pigs with the omentum than in those without it, although there was a steady decrease in the surviving cell number, regardless of the omentum support, as assessed by SPIO cell labeling with CMR and by immunohistolabeling. The pedicle omentum covering markedly increases the number of vessels and capillaries, associated with the upregulation of VEGF, hepatocyte growth factor, and SDF-1, at the transplanted area compared with the cell-sheet transplantation without the omentum.

In the present study, SPIO-labeled hiPS-CMs were clearly visualized in vivo by CMR, corresponding to the histological findings that confirmed iron contents in the transplanted hiPS-CMs that were positive for cTNT, as reported by previous publications.[22,23] Using this method, the distribution and survival of the transplanted hiPS-CMs were serially evaluated in this study. As a result, it was proved that the unique technique in which transplanted cell sheets were covered by the pedicle omentum elicited a greater survival of the transplanted hiPS-CMs over the ventricular epicardial surface at 4 weeks compared with cell-sheet transplantation without the omentum covering. This suggests that pedicle omentum covering the cell sheets promptly induced angiogenesis to improve the hypoxic environment at the transplanted area, compared with the omentum-free method. In addition, although the size of the graft was decreased in both groups during the 8 weeks, trend in the size reduction was significantly milder in the omentum group than in the omentum-free group. This was consistent to the increased vascular network and upregulated angiogenic factors at the transplanted area in the omentum group at 8 weeks after the cell-sheet transplantation. These findings indicate that covering the cell sheet with the pedicle omentum that carries abundant angiogenic potentials[17–19] enhanced neovascular formation at the transplanted area promptly after transplantation and that vascular-rich structure at the transplanted area persisted long-term. In previous studies, antiapoptotic treatments on the transplanted cells, including upregulation of AKT[24] or overexpression of Bcl-2,[25] have been shown to improve survival after cell transplantation. We achieved to improve cell survival after transplantation by modifying the cell delivery method. The pedicled omental flap is frequently and safely applied for the treatment of mediastinitis after cardiovascular surgery. As cell transplantation is indicated to the patients with severe heart failure, we need to establish a minimally invasive approach to mobilize the omentum. Besides, we expect our unique combination method to be a feasible and safe treatment option in clinical settings. However, in this study, transplanted hiPS-CMs produced by our protocol may be immature, although they were spontaneously contractile. In the specimen 8 weeks after transplantation with the omentum, there were few surviving hiPS-CMs with organized sarcomeres in the cytoplasm, whereas there were many cTNT-positive cells (data not shown). In recent studies, mechanical load of hiPS-CMs in vitro controlled their alignment, proliferation, and hypertrophy,[26] and spontaneous and synchronous beating cardiac cell sheets were created by a bioreactor culture, which expanded and induced cardiac differentiation of hiPS cells.[27] It is necessary to modify
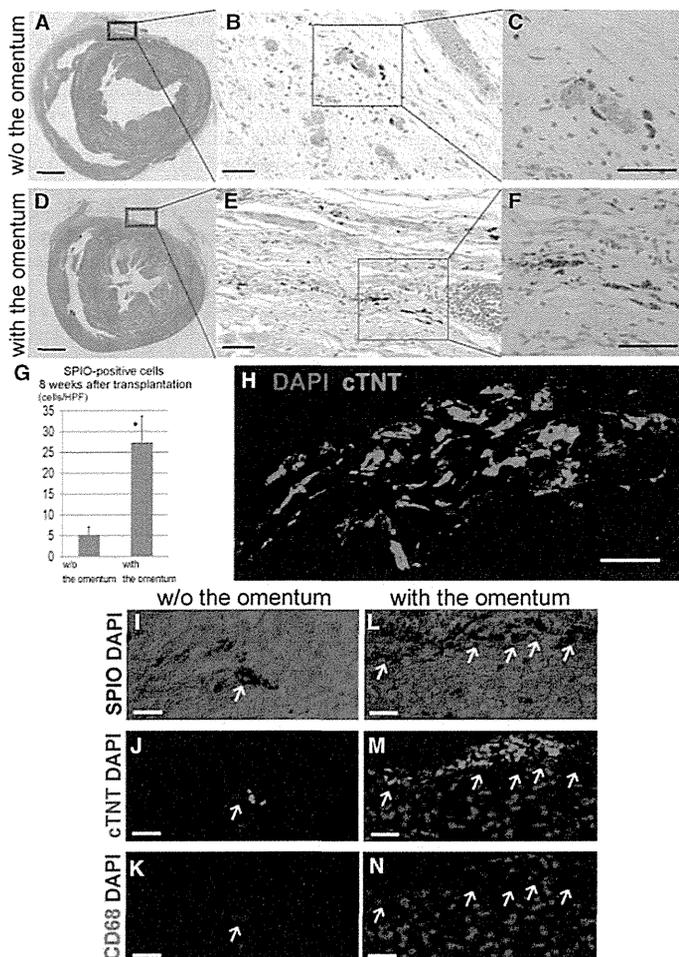
**Figure 4.** Human induced pluripotent stem cell–derived cardiomyocytes (hiPS-CMs) after transplantation. Macroscopic images of the whole heart by hematoxylin–eosin staining at the mid level in the mini-pig without (**A**) or with (**D**) the omentum; scale bar, 1 cm in **A** and **D**. Cells containing iron, indicative of superparamagnetic iron oxide (SPIO)–labeled hiPS-CMs, were detected by Prussian blue staining of sections of mini-pigs without (**B** and **C**) or with (**E** and **F**) the omentum at the transplanted area; scale bar, 50 μm in **B, C, E,** and **F. G,** The density of SPIO-positive cells in the transplanted site was semiquantitatively assessed at 8 weeks after treatment. *$P<0.0001$ vs without the omentum. **H,** In the transplanted regions of mini-pigs with the omentum, cardiac troponin T (cTNT)–positive cells were also demonstrated by immunohistolabeling (green). The cell nuclei were counterstained with 4′,6-diamidino-2-phenylindole (DAPI; blue); scale bar, 50 μm in **H. I–N,** In the transplanted regions of mini-pigs, SPIO particles were visualized by differential interference contrast (DIC), and grafted hiPS-CMs, which were double-positive for cTNT (green) and SPIO (DIC) and negative for CD68 (red), were indentified by immunohistolabeling. The cell nuclei were counterstained with DAPI (blue). Arrows indicate SPIO particles, referred to DIC images in **I** and **L;** scale bar, 20 μm in **I–N.**

our hiPS-CM preparation protocols referred to in these studies to yield the amount of contracting hiPS-CMs contributing to the mechanical function of the injured heart. In addition, we previously demonstrated that maturation of iPS-CMs progressed after iPS-CMs were transplanted in nude rat heart.[28] Therefore, we also expect that improving environments after cell transplantation, such as avoiding delivered cell ischemia, inflammation, and immunogenic rejection, will promote in vivo differentiation of iPS-CMs and their therapeutic effects. The combination of hiPS-CM sheets and the omentum is a promising delivery method to differentiate hiPS-CMs in vivo, because the omentum at least prevents cell ischemia after transplantation and provides better environments.

The cause of reduction in the graft size during the 8 weeks after the cell-sheet transplantation in both groups was not fully addressed in this study. However, one may consider that this reduction was caused by host immune rejection. 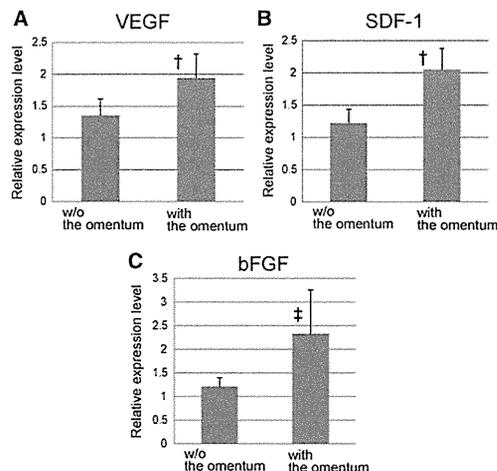We used a combined 3 immunosuppressant regimen, consisting of tacrolimus, mycophenolate mofetil, and corticosteroid, because our experiment was a xenotransplantation model, in which human tissue–derived cells were transplanted in a porcine. In addition, mesenchymal stem cells, which have the potential to induce immunologic tolerance,[29] were involved in creating hiPS-CM cell sheets, and recent studies have reported that the omentum has not only angiogenic cytokines and growth factors but also anti-inflammatory properties and thus can facilitate tissue healing of injured tissue or organs.[30] With our cell delivery method that combines the cell-sheet method with the pedicled omental flap, the 3-drug immunosuppressant regimen, and a mixture of mesenchymal stem cells, it would be difficult to permanently maintain a large number of delivered cells in this xenotransplantation model. Future clinical study of hiPS-CM transplantation for treating heart disease might be performed as allogeneic transplantation.[31] Further studies related to immunologic tolerance are needed to maintain the delivered cells long-term or permanently in this treatment.
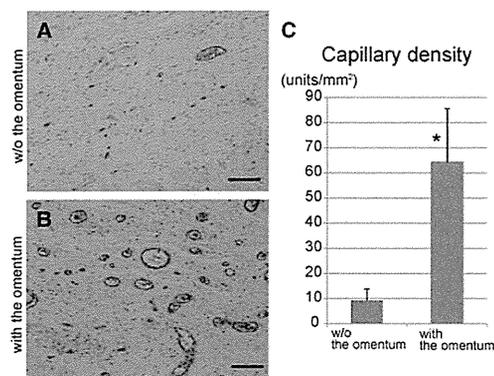
Figure 5. Capillary density in the transplanted area. Photomicrographs of immunostaining for von Willebrand factor are shown in **A** and **B**; scale bar, 50 μm. **C**, The capillary density in the transplanted area was significantly greater in the mini-pigs with the omentum than in those without it. *$P<0.0001$ vs without the omentum.



Figure 6. Angiogenesis-related mRNA expression in the transplanted area, as measured by real-time polymerase chain reaction. Relative expression of angiogenesis-related factors at the transplanted area was significantly greater in mini-pigs with the omentum than in those without it (**A**, vascular endothelial growth factor [VEGF], †$P<0.05$; **B**, stromal-derived factor [SDF]-1, †$P<0.05$; **C**, basic fibroblast growth factor [bFGF], ‡$P<0.01$ vs without the omentum).

In addition, more importantly, hiPS-CM cell sheets were transplanted over the normal epicardium, in which the tissue structure is well organized. New vascular network formation between the native myocardium and the transplanted cell sheets is thus insufficient to support the survival of the transplanted cells, leading to reduction of surviving transplanted cells long-term. In the clinical scenario, however, cell sheets will be transplanted over the diseased heart surface, in which epicardial structure is impaired. Conditions of the host myocardium possibly influence the survival of the transplanted cells. Our results indicate that transplanted cell sheets may provide sufficient blood supply, not from the host myocardium but from the omentum tissue. Thus, we consider that the omentum flap technique could provide a well-organized vascular network, regardless of conditions of the host myocardium, to enhance the survival of the transplanted cells. Further studies are needed to explore the mechanisms underlying integration of the transplanted cells sheets into the heart and to develop methods to enhance the survival and functionality of the transplanted cells.

Cardiac tissue engineering is another strategy that uses stem cells for the treatment of heart failure. One of the major challenges of in vitro engineering techniques is to overcome the limited thickness of the construct because the maximum oxygen diffusion is limited to ≈200 μm². A few recent methodologies have successfully yielded thicker engineered cardiac tissues. Cardiomyocytes in the Matrigel matrix were implanted with an arteriovenous blood vessel loop in vivo, and spontaneously contracting, thick, 3-dimensional constructs with extensive vascularization were thus attained.[32] The cell-sheet method, which is a scaffold-free system, is also an in vitro engineering technique. A cell sheet, itself, has a potential to induce angiogenesis quickly after implantation, and cell-dense 1-mm thick cardiac tissue was developed by repeated transplantation of triple-layered rat neonatal cardiac cell sheets.[33] This cardiac graft generated by this method, however, would be limited in use as a

graft transplanted to the heart because of the lack of responsible large arteries and veins that can be revascularized after transplantation to the heart. In the present study, we used the omentum as a blood supply source after cell transplantation and demonstrated that the omentum enhanced angiogenesis and survival of the delivered cells. In addition, the omentum can easily be handled and mobilized, preserving its vascular network. The omentum, therefore, is a promising tool for in vivo vascularization in cardiac tissue engineering, although further studies with technological development would be needed for this strategy.

In conclusion, covering of the omentum flap over the transplanted hiPS-CM cell sheets on the myocardium effectively promoted angiogenesis, leading to enhanced survival of the hiPS-CMs. These results warrant further investigations as a clinically relevant strategy to enhance hiPS-CM transplantation therapy for heart failure.

## Disclosures
Dr Shimizu is a consultant for CellSeed, Inc. Dr Okano is an Advisory Board Member in CellSeed, Inc, and an inventor/developer designated on the patent for temperature -responsive culture surfaces. The other authors report no conflicts.

# References

1. Menasche P. Cardiac cell therapy: lessons from clinical trials. *J Mol Cell Cardiol.* 2011;50:258–265.
2. Hsiao LC, Carr C, Chang KC, Lin SZ, Clarke K. Stem cell-based therapy for ischemic heart disease. *Cell Transplant.* 2013;22:663–675.
3. Chimenti I, Smith RR, Li TS, Gerstenblith G, Messina E, Giacomello A, Marbán E. Relative roles of direct regeneration versus paracrine effects of human cardiosphere-derived cells transplanted into infarcted mice. *Circ Res.* 2010;106:971–980.
4. Tang XL, Rokosh G, Sanganalmath SK, Yuan F, Sato H, Mu J, Dai S, Li C, Chen N, Peng Y, Dawn B, Hunt G, Leri A, Kajstura J, Tiwari S, Shirk G, Anversa P, Bolli R. Intracoronary administration of cardiac progenitor cells alleviates left ventricular dysfunction in rats with a 30-day-old infarction. *Circulation.* 2010;121:293–305.
5. Takahashi K, Tanabe K, Ohnuki M, Narita M, Ichisaka T, Tomoda K, Yamanaka S. Induction of pluripotent stem cells from adult human fibroblasts by defined factors. *Cell.* 2007;131:861–872.
6. Yu J, Vodyanik MA, Smuga-Otto K, Antosiewicz-Bourget J, Frane JL, Tian S, Nie J, Jonsdottir GA, Ruotti V, Stewart R, Slukvin II, Thomson JA. Induced pluripotent stem cell lines derived from human somatic cells. *Science.* 2007;318:1917–1920.
7. Yoshida Y, Yamanaka S. iPS cells: a source of cardiac regeneration. *J Mol Cell Cardiol.* 2011;50:327–332.
8. Shimizu T, Yamato M, Isoi Y, Akutsu T, Setomaru T, Abe K, Kikuchi A, Umezu M, Okano T. Fabrication of pulsatile cardiac tissue grafts using a novel 3-dimensional cell sheet manipulation technique and temperature-responsive cell culture surfaces. *Circ Res.* 2002;90:e40.
9. Zvibel I, Smets F, Soriano H. Anoikis: roadblock to cell transplantation? *Cell Transplant.* 2002;11:621–630.
10. Memon IA, Sawa Y, Fukushima N, Matsumiya G, Miyagawa S, Taketani S, Sakakida SK, Kondoh H, Aleshin AN, Shimizu T, Okano T, Matsuda H. Repair of impaired myocardium by means of implantation of engineered autologous myoblast sheets. *J Thorac Cardiovasc Surg.* 2005;130:1333–1341.
11. Sekine H, Shimizu T, Dobashi I, Matsuura K, Hagiwara N, Takahashi M, Kobayashi E, Yamato M, Okano T. Cardiac cell sheet transplantation improves damaged heart function via superior cell survival in comparison with dissociated cell injection. *Tissue Eng Part A.* 2011;17:2973–2980.
12. Sawa Y, Miyagawa S, Sakaguchi T, Fujita T, Matsuyama A, Saito A, Shimizu T, Okano T. Tissue engineered myoblast sheets improved cardiac function sufficiently to discontinue LVAS in a patient with DCM: report of a case. *Surg Today.* 2012;42:181–184.
13. Kawamura M, Miyagawa S, Miki K, Saito A, Fukushima S, Higuchi T, Kawamura T, Kuratani T, Daimon T, Shimizu T, Okano T, Sawa Y. Sheets in a porcine ischemic cardiomyopathy model. *Circulation.* 2012;126:S29–S37.
14. O'Shaugnessy L. Surgical treatment of cardiac ischemia. *Lancet.* 1937;232:185–94.
15. Bigelow WG, Basian H, Trusler GA. Internal mammary artery implantation for coronary heart disease. A clinical follow-up study on to eight years after operation. *J Thorac Cardiovasc Surg.* 1963;45:67–79.
16. Aldridge HE, Macgregor DC, Lansdown EL, Bigelow WG. Internal mammary artery implantation for the relief of angina pectoris: a follow-up study of 77 patients for up to 13 years. *Can Med Assoc J.* 1968;98:194–198.
17. Shrager JB, Wain JC, Wright CD, Donahue DM, Vlahakes GJ, Moncure AC, Grillo HC, Mathisen DJ. Omentum is highly effective in the management of complex cardiothoracic surgical problems. *J Thorac Cardiovasc Surg.* 2003;125:526–532.
18. Takaba K, Jiang C, Nemoto S, Saji Y, Ikeda T, Urayama S, Azuma T, Hokugo A, Tsutsumi S, Tabata Y, Komeda M. A combination of omental flap and growth factor therapy induces arteriogenesis and increases myocardial perfusion in chronic myocardial ischemia: evolving concept of biologic coronary artery bypass grafting. *J Thorac Cardiovasc Surg.* 2006;132:891–899.
19. Shudo Y, Miyagawa S, Fukushima S, Saito A, Shimizu T, Okano T, Sawa Y. Novel regenerative therapy using cell-sheet covered with omentum flap delivers a huge number of cells in a porcine myocardial infarction model. *J Thorac Cardiovasc Surg.* 2011;142:1188–1196.
20. Toyoda K, Tooyama I, Kato M, Sato H, Morikawa S, Hisa Y, Inubushi T. Effective magnetic labeling of transplanted cells with HVJ-E for magnetic resonance imaging. *Neuroreport.* 2004;15:589–593.
21. Miyoshi S, Flexman JA, Cross DJ, Maravilla KR, Kim Y, Anzai Y, Oshima J, Minoshima S. Transfection of neuroprogenitor cells with iron nanoparticles for magnetic resonance imaging tracking: cell viability, differentiation, and intracellular localization. *Mol Imaging Biol.* 2005;7:286–295.
22. Kraitchman DL, Heldman AW, Atalar E, Amado LC, Martin BJ, Pittenger MF, Hare JM, Bulte JW. In vivo magnetic resonance imaging of mesenchymal stem cells in myocardial infarction. *Circulation.* 2003;107:2290–2293.
23. Takehara N, Tsutsumi Y, Tateishi K, Ogata T, Tanaka H, Ueyama T, Takahashi T, Takamatsu T, Fukushima M, Komeda M, Yamagishi M, Yaku H, Tabata Y, Matsubara H, Oh H. Controlled delivery of basic fibroblast growth factor promotes human cardiosphere-derived cell engraftment to enhance cardiac repair for chronic myocardial infarction. *J Am Coll Cardiol.* 2008;52:1858–1865.
24. Mangi AA, Noiseux N, Kong D, He H, Rezvani M, Ingwall JS, Dzau VJ. Mesenchymal stem cells modified with Akt prevent remodeling and restore performance of infarcted hearts. *Nat Med.* 2003;9:1195–1201.
25. Li W, Ma N, Ong LL, Nesselmann C, Klopsch C, Ladilov Y, Furlani D, Piechaczek C, Moebius JM, Lützow K, Lendlein A, Stamm C, Li RK, Steinhoff G. Bcl-2 engineered MSCs inhibited apoptosis and improved heart function. *Stem Cells.* 2007;25:2118–2127.
26. Tulloch NL, Muskheli V, Razumova MV, Korte FS, Regnier M, Hauch KD, Pabon L, Reinecke H, Murry CE. Growth of engineered human myocardium with mechanical loading and vascular coculture. *Circ Res.* 2011;109:47–59.
27. Matsuura K, Wada M, Shimizu T, Haraguchi Y, Sato F, Sugiyama K, Konishi K, Shiba Y, Ichikawa H, Tachibana A, Ikeda U, Yamato M, Hagiwara N, Okano T. Creation of human cardiac cell sheets using pluripotent stem cells. *Biochem Biophys Res Commun.* 2012;425:321–327.
28. Yu T, Miyagawa S, Miki K, Saito A, Fukushima S, Higuchi T, Kawamura M, Kawamura T, Ito E, Kawaguchi N, Sawa Y, Matsuura N. In vivo differentiation of induced pluripotent stem cell-derived cardiomyocytes. *Circ J.* 2013;77:1297–1306.
29. Uccelli A, Moretta L, Pistoia V. Mesenchymal stem cells in health and disease. *Nat Rev Immunol.* 2008;8:726–736.
30. Chandra A, Srivastava RK, Kashyap MP, Kumar R, Srivastava RN, Pant AB. The anti-inflammatory and antibacterial basis of human omental defense: selective expression of cytokines and antimicrobial peptides. *PLoS One.* 2011;6:e20446.
31. Pearl JI, Lee AS, Leveson-Gower DB, Sun N, Ghosh Z, Lan F, Ransohoff J, Negrin RS, Davis MM, Wu JC. Short-term immunosuppression promotes engraftment of embryonic and induced pluripotent stem cells. *Cell Stem Cell.* 2011;8:309–317.
32. Morritt AN, Bortolotto SK, Dilley RJ, Han X, Kompa AR, McCombe D, Wright CE, Itescu S, Angus JA, Morrison WA. Cardiac tissue engineering in an in vivo vascularized chamber. *Circulation.* 2007;115:353–360.
33. Shimizu T, Sekine H, Yang J, Isoi Y, Yamato M, Kikuchi A, Kobayashi E, Okano T. Polysurgery of cell sheet grafts overcomes diffusion limits to produce thick, vascularized myocardial tissues. *FASEB J.* 2006;20:708–710.

# Circulation

**American Heart Association®**

## Spatially Oriented, Temporally Sequential Smooth Muscle Cell-Endothelial Progenitor Cell Bi-Level Cell Sheet Neovascularizes Ischemic Myocardium

Yasuhiro Shudo, Jeffrey E. Cohen, John W. MacArthur, Pavan Atluri, Philip F. Hsiao, Elaine C. Yang, Alexander S. Fairman, Alen Trubelja, Jay Patel, Shigeru Miyagawa, Yoshiki Sawa and Y. Joseph Woo

The online version of this article, along with updated information and services, is located on the World Wide Web at:
http://circ.ahajournals.org/content/128/11_suppl_1/S59

# Spatially Oriented, Temporally Sequential Smooth Muscle Cell-Endothelial Progenitor Cell Bi-Level Cell Sheet Neovascularizes Ischemic Myocardium

Yasuhiro Shudo, MD, FAHA; Jeffrey E. Cohen, MD; John W. MacArthur, MD;
Pavan Atluri, MD, FAHA; Philip F. Hsiao, BA; Elaine C. Yang, MS; Alexander S. Fairman, BA;
Alen Trubelja, BS; Jay Patel, BS; Shigeru Miyagawa, MD, PhD; Yoshiki Sawa, MD, PhD;
Y. Joseph Woo, MD, FAHA

***Background***—Endothelial progenitor cells (EPCs) possess robust therapeutic angiogenic potential, yet may be limited in the capacity to develop into fully mature vasculature. This problem might be exacerbated by the absence of a neovascular foundation, namely pericytes, with simple EPC injection. We hypothesized that coculturing EPCs with smooth muscle cells (SMCs), components of the surrounding vascular wall, in a cell sheet will mimic the native spatial orientation and interaction between EPCs and SMCs to create a supratherapeutic angiogenic construct in a model of ischemic cardiomyopathy.

***Methods and Results***—Primary EPCs and SMCs were isolated from Wistar rats. Confluent SMCs topped with confluent EPCs were spontaneously detached from the Upcell dish to create an SMC-EPC bi-level cell sheet. A rodent ischemic cardiomyopathy model was created by ligating the left anterior descending coronary artery. Rats were then immediately divided into 3 groups: cell-sheet transplantation (n=14), cell injection (n=12), and no treatment (n=13). Cocultured EPCs and SMCs stimulated an abundant release of multiple cytokines in vitro. Increased capillary density and improved blood perfusion in the borderzone elucidated the significant in vivo angiogenic potential of this technology. Most interestingly, however, cell fate–tracking experiments demonstrated that the cell-sheet EPCs and SMCs directly migrated into the myocardium and differentiated into elements of newly formed functional vasculature. The robust angiogenic effect of this cell sheet translated to enhanced ventricular function as demonstrated by echocardiography.

***Conclusions***—Spatially arranged EPC-SMC bi-level cell-sheet technology facilitated the natural interaction between EPCs and SMCs, thereby creating structurally mature, functional microvasculature in a rodent ischemic cardiomyopathy model, leading to improved myocardial function. (*Circulation*. 2013;128[suppl 1]:S59–S68.)

**Key Words:** angiogenesis ■ cardiovascular diseases ■ cells ■ endothelium ■ heart failure ■ tissue

Heart failure is the leading cause of death in the United States, with a 5-year mortality of 50%. Current treatment for heart failure entails medical optimization, along with limited revascularization and reconstructive techniques. These interventions do not address the microvascular deficiencies that develop in ischemic cardiomyopathy (ICM). Myocardial regenerative and cellular therapy is attracting growing interest as a means to improve left ventricular (LV) function in advanced heart failure. Among the many candidate cells, endothelial progenitor cells (EPCs), the precursor of blood vessels, have demonstrated excellent potential for therapeutic angiogenesis. Recent reports show beneficial effects of EPC transplantation therapy in several animal experimental models and patients with heart failure.[1-3]

The mechanism by which damaged myocardium is restored by transplanted EPCs is complex and involves many pathways. Recent large-scale clinical trials, in which EPCs were delivered using direct myocardial injection[4] or catheter-based intracoronary procedures,[5,6] reported only modest therapeutic benefits. The limited benefits are at least partially because of poor localized cell survival after transplantation, thereby greatly attenuating the angiogenic potential of EPC therapy. In addition, mature vasculature requires the presence of supporting elements, such as smooth muscle cells (SMCs), which are not delivered with simple EPC injection. In contrast, cell-sheet technology delivers cells more effectively with minimal cell dispersion and myocardial injury and improves microvascular structure, leading to better cardiac function than that attained

by intracoronary injection or needle injection.[7-11] Specifically, the cell-sheet technology enables the construction of a cellular system that mimics the natural architecture of a desired tissue. Here, the proposed angiogenic therapy uses the cell sheet to optimize the spatial arrangement of EPCs and SMCs to maximally induce structurally mature vasculature. The cell sheet is generated on and removed from special dishes that are grafted with a temperature-responsive polymer that changes from hydrophobic to hydrophilic when the temperature is lowered. The greatest advantage of this technique is that the cell sheet consists of densely adherent cells without requiring an artificial scaffold, it is easily manipulated and has a high ability to integrate with native tissues without destroying the cell–cell or cell–extracellular matrix (ECM) adhesions in the cell sheet.[7] In addition, we focused on the concept that the natural endothelial–pericyte spatial relationship and interaction are crucial for vessel maturation and stabilization. Thus, we hypothesized that SMCs, which are components of vascular pericytes, would enhance EPC-mediated angiogenesis and facilitate blood vessel maturation. Neoangiogenesis should yield increased blood perfusion and restoration of cardiomyocyte viability. To demonstrate clear and direct contribution of the cell-sheet EPCs and SMCs to neovasculature, we constructed multiple fate-tracking experiments. A labeled cell sheet was created with EPCs from female rats ubiquitously expressing the enhanced green fluorescent protein (GFP), along with SMCs from male rats. This cell sheet with trackable elements was then implanted in female rats.

In short, this study examined the functional benefits of transplanting the bi-level cell sheet created from cocultured EPCs and SMCs in an ICM model, compared with direct myocardial needle injection.

## Methods

### Isolation of EPCs and SMCs

Wistar rats were administered pentobarbital (100 mg/kg, IP), and then the carotid artery was dissected and transected. Bone marrow mononuclear cells were isolated from the long bones of rats by density gradient centrifugation with Histopaque 1083 (Sigma-Aldrich) and cultured in endothelial basal medium-2 supplemented with EGM-2 SingleQuot (Lonza) containing human epidermal growth factor, 5% fetal bovine serum (Sigma-Aldrich), vascular endothelial growth factor (VEGF), basic human fibroblast growth factor, recombinant human long R3 insulin-like growth factor-1, ascorbic acid, gentamicin, and amphotericin B. The combination of endothelium-specific media and the removal of nonadherent bone marrow mononuclear cells were intended to select for the EPC phenotype. EPCs were cultured for 7 days in the same medium.[2] For EPC fate tracking, we used GFP transgenic female Wistar rats.

SMCs were isolated from the thoracic aorta of wild-type male Wister rats (3 weeks old; Charles River) by primary explant technique[12] and cultured in DMEM with 20% fetal bovine serum, gentamicin, and amphotericin B to confluency for 7 days at 37°C and 5% $CO_2$. For SMC fate tracking, we used male Wistar rats.

### Bi-Level Cell-Sheet Preparation

The SMCs were plated at $1.5 \times 10^5/cm^2$ in a 35-mm Upcell dish, which is grafted with temperature-responsive polymers (CellSeed, Tokyo, Japan), and then cultured in EPC-specific medium. After 24 hours of culture at 37°C and 5% $CO_2$, EPCs were added at $1.5 \times 10^5/cm^2$ onto the Upcell dish, which was already confluent with SMCs. After 24 additional hours in culture, the dishes were transferred to another

incubator, set at 20°C, for 1 hour to release the cultured cells as an intact cell sheet. Under this protocol, confluent SMCs topped with confluent EPCs were spontaneously detached from the plate as a sequentially cocultured and specifically spatially oriented SMC-EPC bi-level cell sheet (Figure 1A).[10,11]

## Production and Release of Cytokines/Chemokines

To demonstrate proangiogenic biological activity, supernatant of the cocultured cells (EPCs: $1.5 \times 10^5/cm^2$, SMCs: $1.5 \times 10^5/cm^2$), EPCs ($3.0 \times 10^5/cm^2$), or SMCs ($3.0 \times 10^5/cm^2$), after being cultured for 24 hours, was centrifuged to remove debris and contaminating cells. Levels of VEGF, hepatocyte growth factor (HGF), transforming growth factor-β (TGFβ), and stromal cell–derived factor 1α (SDF1α) in the culture supernatants were analyzed by ELISA kit (Quantikine, R&D Minneapolis, MN; n=6 in each). ELISA was performed in duplicate.

## Assessment of Cytokine Receptor Expressions by Flow Cytometry

To elucidate the biological impact of cocultured EPCs and SMCs on fetal liver kinase 1 (FLK1) and VEGF receptor 2 (VEGFR2) expression, flow cytometry was used in the EPC or SMC cultured with SMC or EPC using the transwell inserts, supplemented with recombinant VEGF, or media only for 24 hours (n=5 in each). The amount of VEGF was determined based on the results of ELISA. Test samples were incubated for 1 hour at room temperature with either mouse monoclonal anti-FLK1 (Santa Cruz Biotechnology) or rabbit anti-VEGFR2 (Abcam). After washing with cold fluorescence-activated cell sorter buffer, cells were incubated at room temperature
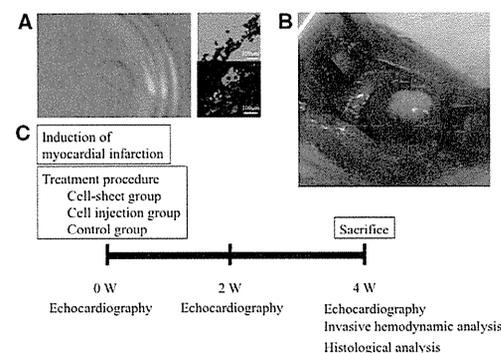


Figure 1. Preparation and transplantation of bi-level cocultured cell-sheet containing both endothelial progenitor cells (EPCs) and smooth muscle cells (SMCs). A, Confluent SMCs topped with confluent EPCs were spontaneously detached from an Upcell dish, which is grafted with temperature-responsive polymers (CellSeed, Tokyo, Japan), as a sequentially cocultured and specifically spatially oriented SMC-EPC bi-level cocultured cell-sheet. Hematoxylin-eosin staining; cross-sectional views of cell-sheet in vitro. Cocultured bi-level cell sheet maintained green fluorescent protein (GFP)-positive EPCs and Y chromosome-positive SMCs in separate layers in vitro. Red indicates rat Y chromosome; green, GFP. B, Bi-level cocultured cell-sheet, which consisted of $1.3 \times 10^6$ EPCs and $1.3 \times 10^6$ SMCs, was placed into the epicardium of the left ventricle covering the ischemic area. C, Study protocol used for assessment of cardiac function and histology. Wistar rats underwent induction of myocardial infarction by occluding the LAD permanently, followed by the concurrent treatment procedure. Cardiac function was assessed by echocardiography just before and at 2 and 4 weeks after the treatment procedure. Four weeks after the treatment procedure, invasive hemodynamic analysis and histological examination were performed after euthanasia.

for 30 minutes with Alexa 647 chicken anti-mouse IgG (Invitrogen) and Alexa 488 donkey anti-rabbit IgG (Invitrogen). The percentage of cells expressing each cell surface antigen was analyzed with a Becton Dickinson FACSCalibur flow cytometer. Data analysis was performed using FlowJo 8.8.3 (Tree Star Inc).[3,13]

## Rat ICM Model and Cell-Sheet Transplantation

Female Wistar rats (8 weeks old, 250–300g; Charles River) were anesthetized with ketamine (75 mg/kg IP) and xylazine (7.5 mg/kg IP), intubated in an endotracheal manner with a 19-gauge catheter, and mechanically ventilated (Hallowell EMC). Anesthesia was maintained by inhalation of 2.0% isoflurane (Clipper Distributing Company Llc, Saint Joseph, MO).

The proximal left anterior descending coronary artery (LAD) of Wistar rats was permanently occluded using a left thoracotomy approach. This produced a consistent and reproducible myocardial infarction encompassing 35% to 40% of the left ventricle.[1-3] Within 5 minutes after LAD ligation, the rats were allocated into 3 groups by simple randomization, considering that there were no differences among the animals at this time point: those that underwent cocultured cell-sheet transplantation (cell-sheet group, n=14), those that underwent cocultured cell injection (cell injection group, n=12), and those that underwent no intervention (control group, n=13). The rats were allowed to recover under care.

In the cell-sheet group, the cocultured bi-level cell sheet, which consists of 1.3×10⁶ EPCs and 1.3×10⁶ SMCs, was placed on the epicardium covering the ischemic area (Figure 1B). The cell injection group received 1.3×10⁶ EPCs and 1.3×10⁶ SMCs, diluted in saline for a total volume of 200 μL by direct intramyocardial injection with a 30-gauge needle. Each rat received the same number of cells. Animals were then kept in temperature-controlled individual cages for 4 weeks.

The rats were euthanized at 4 weeks after surgery by intravenous injection of 200 mg/kg of pentobarbital and 2 mEq/kg of potassium chloride, under terminal anesthesia, and the heart was excised.

## Histological and Immunohistochemical Analyses

Four weeks after treatment, the hearts were dissected and embedded in optimum cutting temperature compound for 10-μm-thick cryosections. The cryosections were used for routine hematoxylin-eosin staining to assess the myocardial structure. Masson trichrome staining was performed to assess cardiac fibrosis in the peri-infarct borderzone. The fibrotic region was calculated as the percentage of myocardial area. The data were collected from 5 individual views per heart at a magnification of ×200. The heart cryosections were also stained with an antibody to von Willebrand factor (vWF; 1:200 dilution; Abcam) to assess capillary density, which was calculated as the number of positively stained capillary vessels in 5 randomly selected fields in the peri-infarct borderzone area, per heart. The cryosections were also stained with an antibody to proliferating cell nuclear antigen (1:200 dilution; Abcam) to assess cellular proliferative activity in 5 randomly selected fields in the peri-infarct borderzone area. The cryosections were also stained with an antibody to integrin β1 (1:100 dilution; Abcam) to estimate cell–matrix attachment in 5 randomly selected fields in the peri-infarct borderzone area. Cell nuclei were counterstained with 6-diamidino-2-phenylindole (Invitrogen). The images were examined by fluorescence microscopy (Leica). Image J software was used for quantitative morphometric analysis.

## EPC-SMC Fate Tracking

The cell sheet, which consisted of EPCs from GFP transgenic female Wistar rats and SMCs from non-GFP male Wistar rats, was transplanted into the female Wistar rat heart. To detect the fate of EPCs, cryosections were stained with an anti-vWF antibody (1:1000 dilution; Abcam), anti–smooth muscle actin (SMA) antibody (1:1000 dilution; Abcam), anti–vascular endothelial-cadherin antibody (1:1000 dilution; Santa Cruz), and anti-GFP antibody (1:1000 dilution; Abcam). The secondary antibodies were Alexa Fluor 555 donkey anti-rabbit IgG (1:1000 dilution; Invitrogen) and Alexa Fluor

555 donkey anti-mouse IgG (1:1000 dilution; Invitrogen). To detect the fate of SMCs, fluorescence in situ hybridization was performed on cryosections, which were then stained with anti-SMA antibody (1:500 dilution; Abcam). The secondary antibody was Alexa Fluor 555 donkey anti-rabbit IgG (1:500 dilution; Invitrogen). Cell nuclei were counterstained with 6-diamidino-2-phenylindole. GFP-positive cells and rat Y chromosome–positive cells were counted, respectively, and corrected by total number of tissue cells to estimate the survival cells quantitatively. GFP- and vWF-positive cells were counted and corrected by total number of GFP-positive cells to examine vascular regeneration. Rat Y chromosome– and SMA-positive cells were counted and corrected by total number of rat Y chromosome–positive cells to examine vascular regeneration.

## Myocardial Perfusion Analysis

To quantify myocardial perfusion, at 4 weeks after treatment 200 μg of fluorescein-labeled *Lycopersicon esculentum* (tomato) lectin (Vector Laboratories) was injected into the supradiaphragmatic inferior vena cava and allowed to circulate for 10 minutes. After lectin perfusion, the hearts were explanted and snap-frozen in liquid nitrogen. One-hundred twenty sequential images were obtained through 100-μm thick myocardial sections at the level of the papillary muscle using scanning laser confocal microscopy (z-series, ×20 air magnification, Zeiss LSM-510 Meta Confocal Microscope). Three-dimensional reconstructions of the image stacks were created using Velocity Software v.3.61 (Improvision). Fluorescein-labeled voxels were quantified as a percentage of total tissue section voxels, creating a quantifiable measurement of perfusion per unit of myocardial tissue volume.[2,3]

## Echocardiographic Assessment

Echocardiography was performed under general anesthesia using 1.0% inhaled isoflurane just before and at 2 and 4 weeks after the treatment procedure (SONOS 7500, Philips Medical Systems, Andover, MA) with a 12-MHz transducer at an image depth of 2 cm (cell sheet, n=7; cell injection, n=8; control, n=9; Figure 1C). LV end-diastolic diameter (LVEDD), LV end-systolic diameter (LVESD), and end-diastolic anterior wall thickness at the level of the papillary muscles were measured for ≥3 consecutive cardiac cycles following the American Society for Echocardiology leading-edge method. Fractional shortening (FS) and ejection fraction (EF) were calculated as parameters of systolic function.[2,3,8] All analyses were performed by a single investigator in a group-blinded fashion.

## Invasive Hemodynamic Assessment

Four weeks after the treatment procedure, animals (cell-sheet, n=6; cell injection, n=6; control, n=8) underwent invasive hemodynamic measurements with a pressure–volume conductance catheter (SPR-869; Millar Instruments, Inc; Figure 1C). The catheter was calibrated via 5-point cuvette linear interpolation with parallel conductance subtraction by the hypertonic saline method.[2,3] Rats were anesthetized using 1.0% inhaled isoflurane, and the catheter was introduced into the LV with a closed-chest approach via the right carotid artery. Measurements were obtained before and during inferior vena cava occlusion to produce static and dynamic pressure–volume loops under varying load conditions. Data were recorded and analyzed with LabChart version 6 software (AD Instruments) and ARIA Pressure Volume Analysis software (Millar Instruments, Inc). After hemodynamic assessment, the heart was removed for further histological analyses.

## Statistical Analysis

Continuous variables are expressed as mean±SE. Comparisons between 2 groups were made using the Wilcoxon–Mann–Whitney $U$ test because of small sample sizes. For comparisons among 3 groups, we used the Kruskal–Wallis test, followed by the post hoc pairwise Wilcoxon–Mann–Whitney $U$ test. The multiplicity in pairwise comparisons was corrected by the Bonferroni procedure. A $P<0.05$ was

considered statistically significant. All statistical calculations were performed using SPSS software (version 11.0; SPSS Inc, Chicago, IL) and JMP 9.0 (SAS Institute Inc, Cary, NC).

### Animal Care and Biosafety

Wistar rats were obtained from Charles River. Food and water were provided ad libitum. This investigation conforms with the Guide for the Care and Use of Laboratory Animals published by the US National Institutes of Health (NIH Publication No. 85-23, revised 1996) and was approved by the Institutional Animal Care and Use Committee of the University of Pennsylvania (protocol 803394).

## Results

### Production and Release of Cytokines/Chemokines by Coculturing EPC With SMC

VEGF was significantly higher in the coculture supernatant than the SMC-only group and tended to be higher than the EPC-only group (Figure 2A). The secretion of HGF was remarkably enhanced in the coculture supernatant, whereas HGF levels were not evident in either the EPC- or SMC-alone group (Figure 2B). The concentration of TGFβ was significantly higher in the coculture supernatant than both the EPC- and SMC-only groups (Figure 2C). The secretion of SDF1α was remarkably higher in the cocultured group compared with EPC and SMC alone (Figure 2D).

### Upregulated Expressions of FLK1 and VEGFR2 on Either EPC or SMC Under Cytokines-Rich Medium of SMC or EPC

Flow cytometric analysis demonstrated that the percentage of FLK1+ EPCs and VEGFR2+ EPCs in total EPC population was 1.3±0.3% and 3.2±0.8%, respectively. Supplementation with VEGF significantly increased the percentage of FLK1+ EPCs (17.2±3.2%) and VEGFR2+ EPCs (32.0±5.4%). Furthermore, the percentage of FLK1+ and VEGFR2+ EPCs was significantly greater after coculturing with SMC (FLK1+, 39.6±9.2%; VEGFR2+, 52.5±9.8%; Figure 3A and 3B).

Flow cytometric analysis demonstrated a statistically significant increase in the percentage of FLK1+ SMCs cocultured with EPC compared with SMC alone (75.7±5.4 versus 23.9±2.5%; P=0.02). Addition of VEGF significantly

increased FLK1+ SMCs compared with SMC (Figure 3C and 3D). There was no significant difference in the VEGFR2+ expression on SMCs (P=0.14, Kruskal–Wallis test).

### Enhanced Capillary Density and Microvascular Perfusion After Cocultured Cell-Sheet Transplantation

A large number of vWF-positive blood vessels were detected in the peri-infarct borderzone myocardium after cell-sheet therapy compared with injection alone (Figure 4A). This demonstrated a superior enhancement of capillary density in the cell-sheet group (Figure 4B).

Similarly, lectin microangiography of the peri-infarct borderzone myocardium sections revealed a more densely and well-developed capillary network in the cell-sheet group compared with injection alone (Figure 4C). Quantitative analysis showed significantly enhanced perfusion in the peri-infarct borderzone myocardium in the cell-sheet group (Figure 4D).

### Enhanced Cell Proliferation Activity After Cocultured Cell-Sheet Transplantation

A large number of proliferating cell nuclear antigen-positive cells were identified in the peri-infarct borderzone myocardium after cell-sheet therapy compared with control (Figure 4E and 4F).

### Migration of EPCs and SMCs to Myocardium Contributing to Neovasculature

Cocultured bi-level cell sheet contained GFP-positive EPCs and Y chromosome–positive SMCs in separate layers in vitro (Figure 1A).

Four weeks after transplantation, the GFP-positive EPCs were detected in the myocardium at the transplanted site at an appropriate depth of 650 μm (Figure 4G). Immunostaining for vWF and GFP showed that transplanted EPCs were able to contribute to neovascularization of the host myocardium (Figure 4H). This was further supported by immunostaining for vascular endothelial-cadherin and GFP (Figure 4I). In addition, staining with antibody to SMA and GFP indicated that GFP-positive EPCs originating from the transplanted cocultured bi-level cell sheet migrated into the engineered
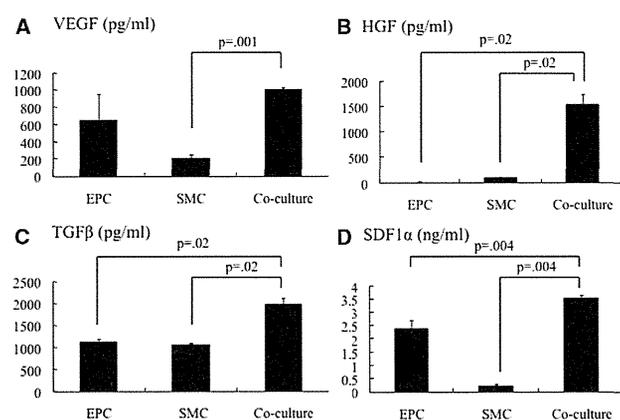


Figure 2. A, Vascular endothelial growth factor (VEGF), (B) hepatocyte growth factor (HGF), (C) transforming growth factor-β (TGFβ), and (D) stromal cell–derived factor 1α (SDF1α) in the culture supernatant, measured by ELISA. Cocultured endothelial progenitor cells (EPCs) with smooth muscle cells (SMCs) secreted abundant VEGF, HGF, TGFβ, and SDF1α compared with either EPC or SMC (n=6 in each; VEGF, P=0.002; HGF, P=0.01; TGFβ, P=0.01; SDF1α, P=0.001; Kruskal–Wallis test).
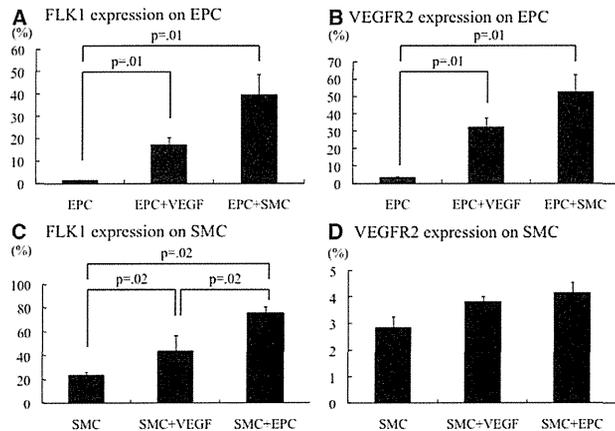
**Figure 3.** To elucidate the biological impact of cocultured endothelial progenitor cell (EPC)-smooth muscle cells (SMCs) on FLK1 and vascular endothelial growth factor receptor 2 (VEGFR2) expression, flow cytometry was used to study both EPC and SMC expression of these markers in the following settings: cocultured, cultured with VEGF, and cultured alone. The amount of VEGF used was determined based on the results of ELISA. A and B, The percentage of FLK1⁺ EPC and VEGFR2⁺ EPC was greatest in a cocultured setting (n=5 in each; FLK1 expression on EPC, $P$=0.01; VEGFR2 expression on EPC, $P$=0.01; Kruskal–Wallis test). C and D, Analysis of SMC FLK1⁺ expression demonstrated a significant increase in the cocultured group. There was no significant difference in the VEGFR2⁺ expression on SMC (n=4 in each; FLK1 expression on SMC, $P$=0.01; VEGFR2 expression on SMC, $P$=0.14; Kruskal–Wallis test).

myocardial tissues and were circumferentially surrounded by SMA-positive tissues (Figure 4J). Finally, to track SMCs from the cell sheet, we performed fluorescence in situ hybridization immediately to identify male SMCs in the female recipient. After the cell-sheet transplantation, GFP-positive EPCs and Y chromosome–positive SMCs were detected with a thickness of ≈50 μm into the epicardium (Figure 4K). Rat Y chromosome SMCs were partially able to differentiate into SMA-positive tissues (Figure 4L). Quantitative analysis showed a greater percentage of GFP-positive cells and rat Y chromosome–positive cells, respectively, in the cell-sheet group compared with cell injection (Figure 4M). Quantitative analysis of vascular regeneration showed that the number of both GFP- and vWF-positive cells is 18±3/hpf (60% of GFP-positive cells), which participated in new blood vessel formation. In addition, the number of both Y chromosome– and SMA-positive cells is 7±2/hpf (45% of rat Y chromosome cells), which participated in new blood vessel formation. One week after treatment, a large number of integrin β1–positive cells were observed in the peri-infarct borderzone myocardium after cell-sheet therapy compared with cell injection and control (Figure 4N and 4O).

### LV Remodeling After Cell-Sheet Transplantation

The LV myocardial structure was superiorly maintained after cell-sheet transplantation compared with cell injection and control, as assessed by hematoxylin-eosin staining (Figure 5A). In addition, cell-sheet therapy significantly attenuated collagen accumulation in the infarct area compared with cell injection and control, as demonstrated by Masson trichrome staining (Figure 5B and 5C).

### Cardiac Functional Recovery After Cell-Sheet Transplantation

The effects of cocultured bi-level cell-sheet transplantation on cardiac function were assessed in a rat ICM model. After permanent occlusion of the LAD, EF, FS, and anterior wall thickness (baseline, 1.7±0.1 mm; at 2 weeks, 0.8±0.1 mm, at 4 weeks, 0.8±0.1 mm; $P$=0.0001, Kruskal–Wallis test) showed steady reductions, whereas EDD/ESD showed steady

increases (EDD, $P$=0.0002; ESD, $P$=0.0001; Kruskal–Wallis test), suggesting progressive LV remodeling. After cocultured cell injection, the heart showed mild recovery, including increases in FS and EF. At 4 weeks after treatment, EF and FS tended to be greater after cocultured cell injection than the control; however, an even greater recovery was observed after cell-sheet transplantation (Figure 6A and 6B). At 4 weeks, the bi-level cell-sheet group had a significantly greater EF and FS and significantly improved EDD and ESD compared with either cell injection or control (Figure 6C and 6D).

Assessment by pressure–volume catheter further confirmed the cell-sheet–induced functional enhancement demonstrated by the echocardiographic data. Four weeks after transplantation, the maximal rate of change in LV pressure (max. dP/dt) and end-systolic pressure–volume relationship were significantly enhanced in the cell-sheet group compared with cell injection and control (Figure 7). Mimimal rate of change in LV pressure (min. dP/dt) and cardiac output were higher in the cell-sheet group than the other 2 groups, but the difference was not significant.

### Discussion

This study revealed a multifaceted mechanism by which the targeted implantation of an EPC-SMC bi-level cell-sheet enhances myocardial function in a rodent model of ICM. A significant chemokine effect was observed in vitro where cocultured EPC-SMCs stimulated an abundant release of SDF1α, VEGF, HGF, and TGFβ; this effect is a mechanistic component of the augmented angiogenesis demonstrated in vivo. More importantly, however, the data clearly established direct migration of the cell-sheet EPCs and SMCs into the myocardium and confirmed these cells to be some elements of newly formed functional vasculature. The observed increased capillary density and improved blood perfusion in the borderzone elucidated the significant in vivo angiogenic potential of this technology. Furthermore, cell fate–tracking experiments strongly suggested the cell-sheet EPCs and SMCs as components of newly assembled vasculature. With regard to cell engraftment, the cell-sheet group performed superiorly, demonstrating improved cell–matrix attachment compared
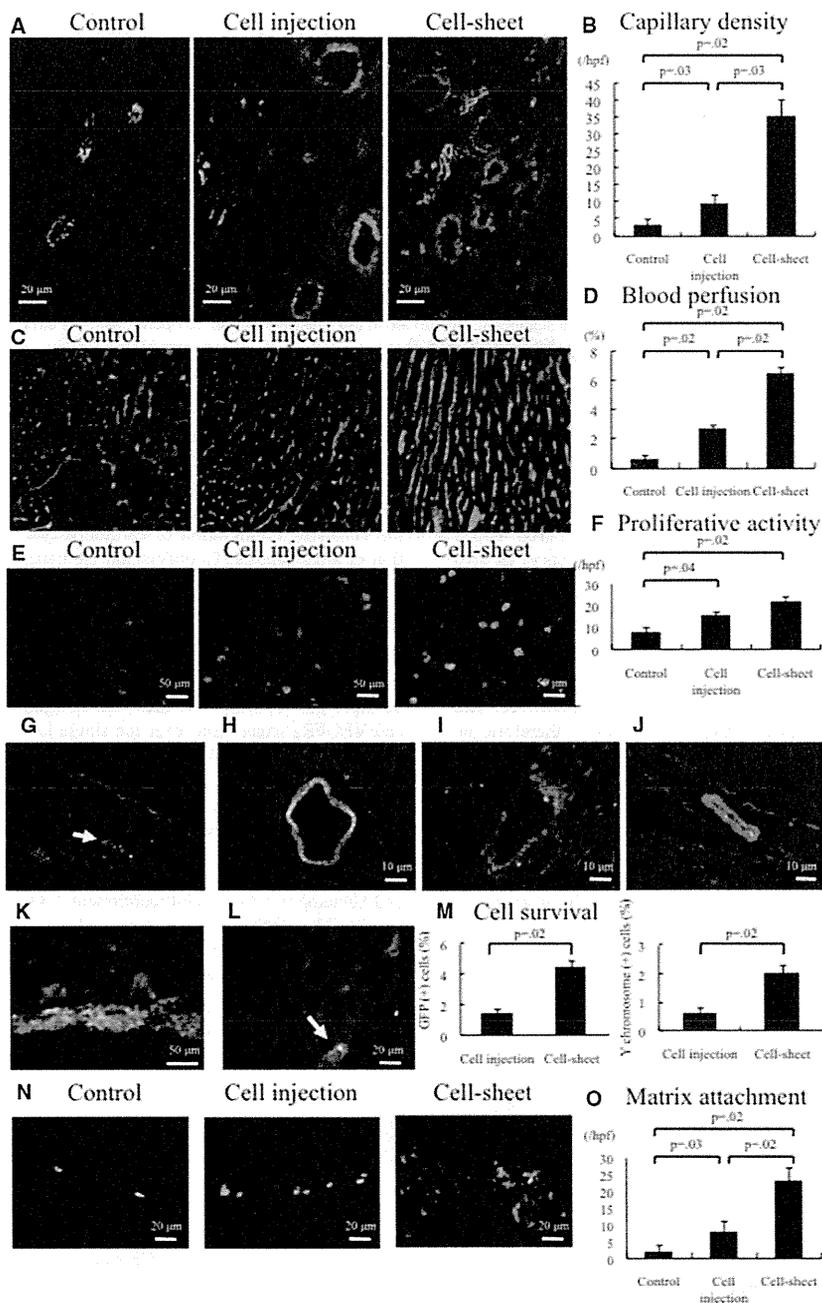
Figure 4. Effects on left ventricular remodeling, capillary density, and microvascular perfusion by bi-level cocultured cell-sheet transplantation (cell-sheet), cocultured cell injection (cell injection), and control (control) 4 weeks after the treatment procedure. **A**, Representative von Willebrand factor (vWF) staining of the borderzone myocardium. **B**, Quantification of capillary density. Capillary density was significantly enhanced in the cell-sheet groups compared with other groups (cell-sheet, n=4; cell injection, n=3; control, n=4; $P$=0.01, Kruskal–Wallis test). **C**, Representative lectin microangiographic imaging from the borderzone myocardium (×20 magnification). **D**, Quantitative analysis showed enhanced blood perfusion in the cell-sheet group compared with the other groups (cell sheet, n=4; cell injection, n=4; control, n=4; $P$=0.01, Kruskal–Wallis test). **E**, Representative antiproliferative cell nuclear

*(Continued)*

**Figure 4. Continued** antigen staining of the borderzone myocardium. **F,** Quantification of cell proliferative activity. Proliferative activity was significantly enhanced in the cell-sheet group compared with control (cell sheet, n=4; cell injection, n=4; control, n=4; $P$=0.02, Kruskal–Wallis test). **G,** Immunoconfocal microscopy demonstrated abundant green fluorescent protein (GFP)-positive cells in the myocardium. **H,** Cryosections were stained with an antibody to vWF and GFP to detect the fate of endothelial progenitor cells (EPCs) in the heart. Immunostaining for vWF and GFP showed that transplanted EPCs over the borderzone myocardium were able to contribute directly to neovascularization of the host myocardium. Green indicates GFP; red, vWF; blue, nuclei. **I,** Immunostaining for vascular endothelial (VE)-cadherin and GFP showed that transplanted EPCs were able to contribute to neovascularization of the host myocardium. Green indicates GFP; red, VE-cadherin; blue, nuclei. **J,** In addition, staining with antibody to smooth muscle actin (SMA) and GFP demonstrated that GFP-positive EPCs originating from the transplanted bi-level cell sheet migrated into the treated myocardial tissues and were circumferentially supported by SMA-positive tissues. Green indicates GFP; red, SMA; blue, nuclei. **K,** Furthermore, to track SMCs from the cell sheet, we performed fluorescence in situ hybridization to identify male SMCs in the female recipient. Immediately after the cell-sheet transplantation, GFP-positive EPCs and Y chromosome-positive SMCs were detected in the epicardium. Red indicates rat Y chromosome; green, GFP. **L,** Rat Y chromosome SMCs were able to differentiate into SMA-positive tissues (white arrow). Red indicates SMA; yellow, rat Y chromosome; blue, nuclei. **M,** Quantitative analysis of cell survival estimation. *GFP-positive cells and rat Y chromosome–positive cells were counted, respectively, and corrected by total number of tissue cells to examine the survival cells quantitatively.* **N,** Representative anti–integrin β1 staining of the borderzone myocardium. **O,** Quantification of cell–matrix attachment. Cell–matrix attachment was significantly enhanced in the cell-sheet group compared with the other groups (cell sheet, n=4; cell injection, n=4; control, n=4; $P$=0.01, Kruskal–Wallis test).

with injection alone. The robust angiogenic effect of bi-level cell-sheet translated to enhanced myocardial function of the ischemic heart.

Our group has investigated the effects of EPCs as a neovasculogenic therapy for ICM using EPC therapy alone,[14] with seeded EPCs,[13] and with a tissue-engineered matrix.[2] Based on these findings, we began to explore the effects of ex vivo expanded EPCs. Systemic and direct myocardial injection of EPCs, however, is fraught with complications, such as cell dispersion and high percentages of cell loss. In this study, we used cell-sheet technology, which allows efficient delivery of cells onto the ischemic area of myocardium with minimal myocardial injury and cell dispersion, preserves cell–cell and cell–ECM architectural structure, and might, therefore, be more applicable to human translation.[15]

Given our previous work and experience with cell-sheet technology, one possible mechanism is likely to include cytokine release and hematopoietic stem cell recruitment.[7–9] Previous studies have shown that EPCs acted as the natural supplier of SDF1α,[16] VEGF,[17] HGF,[18] and TGFβ.[19] Their roles and signaling pathways have been intensively investigated; SDF1α is related to cell migration, proliferation, and migration[2,13,16]; VEGF is critical to stimulate endothelial cell proliferation and migration to initiate neovascularization[19]; HGF

is beneficial to an impaired heart and is associated with an antifibrotic effect.[7,20] Together with our findings, it is reasonable to conclude that coculturing EPCs with SMCs enhanced the secretion of cytokines, such as SDF1α, VEGF, HGF, and TGFβ, compared with either EPCs or SMCs, thus leading to the enhanced proliferation of cardiomyocytes and stimulation of angiogenesis. To understand the detailed mechanism by which coculturing enhances cytokine secretion, we performed additional investigations from a new perspective. We found that FLK1 and VEGFR2 were upregulated by additional VEGF, which were even more enhanced by numerous cytokines containing cell-culturing medium, suggesting that multiple growth factors evoked the upregulation of FLK1 and VEGFR2 expressions over the single factor (ie, VEGF), thereby possibly amplifying VEGF release. The understanding of our results may be translated into the emerging concept that SMCs support the biological aspects of EPCs via the endothelial–pericyte cytokine cross-communication.

The mechanism of restoration of damaged myocardium by EPC transplantation is complex.[2,3,13] Although cytokine release and hematopoietic stem cell recruitment have been proposed as possible mechanisms of regeneration, other important mechanisms are likely to be involved. The creation of mature, stable, and functional vessels is essential. It has been reported
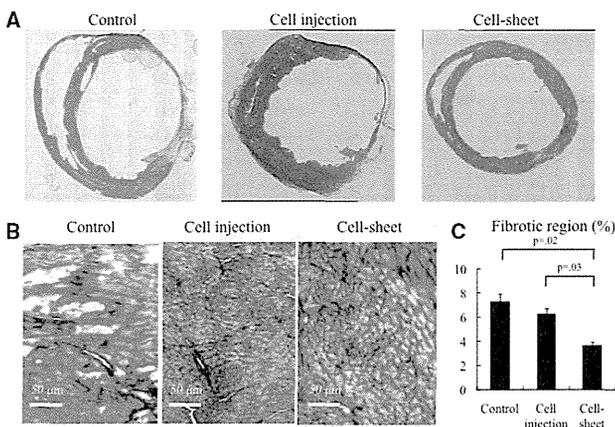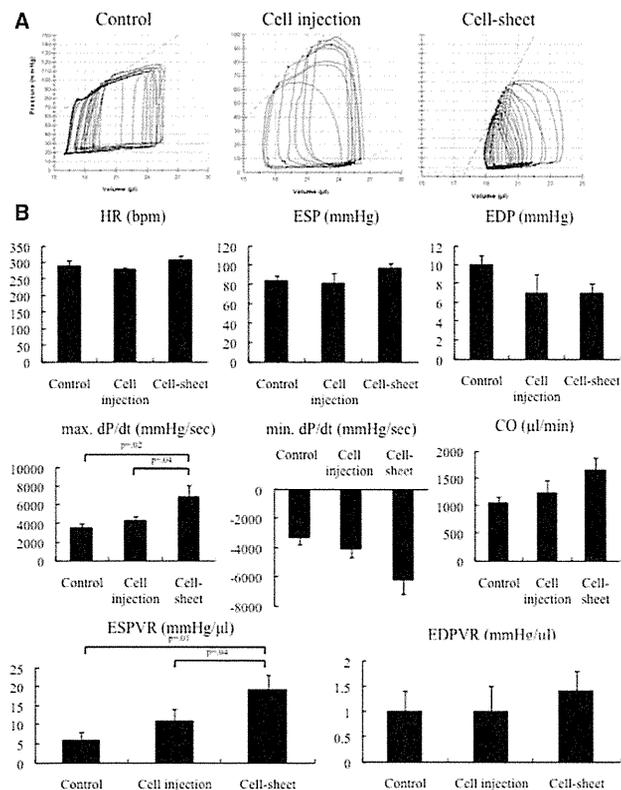


Figure 5. **A,** Representative macroscopic views of the heart (hematoxylin-eosin staining). The myocardial structure was superiorly maintained after cell-sheet transplantation compared with cell injection and control. **B,** Representative Masson trichrome staining at the borderzone myocardium. **C,** Quantification of fibrotic region. Fibrosis at the borderzone area was significantly suppressed in the cell-sheet group compared with the other groups (cell sheet, n=4; cell injection, n=3; control, n=4; $P$=0.02, Kruskal–Wallis test).

**A** EF (%)

**B** FS (%)



**C** EDD (mm)

**D** ESD (mm)
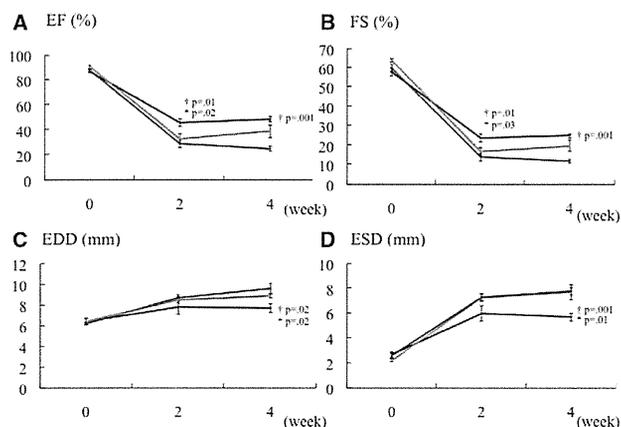
Figure 6. Serial changes in (A) ejection fraction (EF), (B) fractional shortening (FS), (C) end-diastolic diameter (EDD), and (D) end-systolic diameter (ESD) assessed by echocardiography (cell sheet, n=7, black line; cell injection, n=8, red line; control, n=9, blue line). Examinations were performed before (0) and at 2 and 4 weeks of follow-up after the operation. EF and FS were significantly higher at 2 and 4 weeks in the cell-sheet group compared with either cell injection or control (EF at 2 weeks, P=0.01; EF at 4 weeks, P=0.003; FS at 2 weeks, P=0.01; FS at 4 weeks, P=0.003; Kruskal–Wallis test). EDD and ESD were lowest at 4 weeks in the cell-sheet group (EDD, P=0.02; ESD, P=0.003; Kruskal–Wallis test). *P<0.05 vs cell injection; †P<0.05 vs control, post hoc pairwise Wilcoxon–Mann–Whitney U test.

that capillary formation occurs via two basic vessel-constructing processes: angiogenesis (ie, the formation of new capillaries via sprouting or intussusception from preexisting vessels) and vasculogenesis (ie, de novo formation of vasculature as occurs in the developing embryo).[21] It has also been reported that angiogenesis requires a dynamic temporally and spatially regulated interaction among endothelial cells, pericytes, and

angiogenic factors.[22] Given the natural relationship between endothelium and intima within mature vessels, we added SMCs, which are essentially vascular pericytes, to enhance the angiogenic performance of EPCs. Thus, it was hypothesized that coculturing EPCs with SMCs would promote a robust angiogenic response and induce formation of mature blood vessels. Our present study shows that in addition to the

**A** Control — Cell injection — Cell-sheet



**B** HR (bpm) — ESP (mmHg) — EDP (mmHg)



max. dP/dt (mmHg/sec) — min. dP/dt (mmHg/sec) — CO (μl/min)



ESPVR (mmHg/μl) — EDPVR (mmHg/μl)



Figure 7. Hemodynamic measurements determined using cardiac catheterization after cocultured bi-level cell-sheet transplantation (cell-sheet, n=6), cocultured cell injection (cell injection, n=6), and control (control, n=8). Examinations were performed at 4 weeks of follow-up after the operation. A, Representative pressure–volume loops during inferior vena cava occlusion from cell-sheet, cell injection, and control groups. B, There was no significant difference in heart rate (HR), end-systolic pressure (ESP), end-diastolic pressure (EDP), mimimal rate of change in left ventricular (LV) pressure (min. dP/dt), cardiac output (CO), or end-diastolic pressure–volume relationship (EDPVR; HR, P=0.35; ESP, P=0.19; EDP, P=0.14; min. dP/dt, P=0.05; CO, P=0.07; EDPVR, P=0.70; Kruskal–Wallis test). The maximal rate of change in LV pressure (max. dP/dt) and end-systolic pressure–volume relationship (ESPVR) significantly improved in the cell-sheet group compared with the other 2 groups (max. dP/dt, P=0.04; ESPVR, P=0.03; Kruskal–Wallis test).